energies

MDPI

Review

A Review of Biomass-Derived UV-Shielding Materials for Bio-Composites

Tae Hoon Kim [1], Seung Hyeon Park [2], Seoku Lee [3], A.V.S.L. Sai Bharadwaj [2], Yang Soo Lee [4], Chang Geun Yoo [3,*] and Tae Hyun Kim [2,5,*]

1 R&D Center, SugarEn Co., Ltd., Yongin 16890, Gyeonggi-do, Republic of Korea
2 Department of Materials Science and Chemical Engineering, Hanyang University, Ansan 15588, Gyeonggi-do, Republic of Korea
3 Department of Chemical Engineering, State University of New York College of Environmental Science and Forestry, Syracuse, NY 13210, USA
4 Samwon Industrial Co., Ltd., Ansan 15612, Gyeonggi-do, Republic of Korea
5 Namu BioChem Inc., Ansan 15588, Gyeonggi-do, Republic of Korea
* Correspondence: cyoo05@esf.edu (C.G.Y.); hitaehyun@hanyang.ac.kr (T.H.K.); Tel.: +1-(315)-470-6516 (C.G.Y.); +82-(31)-400-5222 (T.H.K.)

Abstract: The adverse effects of UV (ultraviolet) radiation on polymeric materials and organic constituents can damage the molecular structure of human skin and polymeric materials, resulting in their degradation. Therefore, additives or reagents for UV-shielding must be used in related applications, including polymer compounds and skin cosmetics. Bio-based polymers have shown great potential as alternatives to conventional metallic and organic materials (e.g., TiO_2 and ZnO) in various applications; therefore, natural products have gained attention as a potential resource to overcome UV-induced health and environmental problems. In particular, biomass-derived materials such as lignin, fiber, and silica have been investigated as UV-shielding materials owing to their biocompatibility, biodegradability, and low carbon emissions. In this review, the UV-shielding effect and potential of various biomass-derived materials, such as silica, nanocellulose, and fibers, are reviewed. Among them, lignin is considered a promising UV-shielding material because of the presence of chromophores and functional groups capable of absorbing UV radiation of all ranges.

Keywords: lignocellulosic biomass; UV-shielding; polyphenol; biopolymer; bioproduct; bio-based polymer

Citation: Kim, T.H.; Park, S.H.; Lee, S.; Bharadwaj, A.S.; Lee, Y.S.; Yoo, C.G.; Kim, T.H. A Review of Biomass-Derived UV-Shielding Materials for Bio-Composites. *Energies* **2023**, *16*, 2231. https://doi.org/10.3390/en16052231

Academic Editors: Shashi Kant Bhatia and Alberto Coz

Received: 25 January 2023
Revised: 4 February 2023
Accepted: 23 February 2023
Published: 25 February 2023

1. Introduction

The negative effects of UV (ultraviolet) radiation on polymeric materials and organic constituents have been well-documented in numerous studies. Excessive UV exposure damages the molecular structure of all materials, including human skin and polymeric materials, resulting in quality degradation, such as degradation of mechanical properties and reduction in molecular weight (M_w) [1–6]. Generally, UV rays are divided into three categories based on their wavelengths: UVA (315–390 nm), UVB (280–315 nm), and UVC (100–280 nm). UVA can be further subdivided into UVA1 (340–400 nm) and UVA2 (320–340 nm). UV rays can be absorbed by oxygen and stratospheric ozone as they pass through the Earth's atmosphere, but this absorption is wavelength-dependent [7,8]. The most energetic UVC radiation is completely absorbed by ozone without reaching the Earth's surface, while approximately 5–10% of UVB radiation and most UVA radiation pass through the atmosphere [9]. Although UVA and UVB have lower energies than UVC, they penetrate the human epidermis and cause various diseases and skin aging. In particular, UVA penetrates the human dermis and promotes the generation of reactive oxygen species, causing DNA damage, lipid peroxidation, and protein cross-linking, leading to erythema, sunburn, and even skin cancer [10].

Using UV-protective additives or materials is inevitable to protect polymeric materials and human skin from UV radiation. UV has a higher energy than visible light, and the physical properties of most polymer resins change when exposed to UV rays due to photolysis; for example, a photochemical reaction leads to polymer oxidation and color change. Therefore, an appropriate UV stabilizer is usually used to prevent the deterioration of physical properties. Generally, two types of UV stabilizers are used: UV absorbers and hindered amine light stabilizer (HALS)-based compounds. For example, when the benzotriazole compound absorbs UV, electrons move from the phenolic oxygen to the nitrogen atom (keto form) and then drop energy levels by releasing heat (keto-enol tautomerism) [11,12]. On the other hand, HALS-based compounds do not absorb UV light, but remove free radicals generated by photooxidation of polymers and return to their initial form through additional reactions [13,14]. These stabilizers extend the life of the polymer by reducing photodegradation by UV. UV filters can be divided into two types (organic and inorganic) based on the mechanism of protection of the skin from UV rays. Organic filters convert the absorbed light energy and release it as thermal energy to prevent skin damage [15–18] (Figure 1). In contrast, inorganic filters are mineral-based particles that absorb UV radiations and physically block them by reflection and scattering [18,19]. The US Food and Drug Administration (FDA) has approved the use of 14 organic filters and two inorganic filters as active ingredients with prescribed concentration limits for use in over-the-counter (OTC) drugs (Table 1) [20]. They absorb, reflect, or scatter UV radiation in the wavelength range of 290–400 nm. Each active ingredient affects a specific wavelength among the three wavelength ranges of UVA1, UVA2, and UVB. The active ingredients of organic filters provide excellent UV protection, but prolonged use of these substances can cause irritant and allergic contact reactions, as well as photoallergic and phototoxic effects [18,21–24]. In addition, due to the high lipophilicity of organic UV filters, they easily penetrate the human skin and biologically accumulate in organs such as the liver and brain [25]. Accumulated chemicals can act as endocrine disruptors within the human body, causing neurotoxic effects such as decreased neurotransmission and impaired synaptic plasticity [25,26]. The metal oxides zinc oxide (ZnO) and titanium dioxide (TiO_2) are the most representative active components of inorganic filters and effectively reflect and scatter UV light in all wavelength ranges [21,27]. In addition, unlike organic filters, they do not cause skin toxicity or allergy; therefore, they are preferred by users with sensitive skin [18,21,24]. In the market, metal oxides are supplied in micronized forms, which do not scatter visible light and retain the natural look of the skin after application. For the skin to appear natural, the size of the inorganic material must be small; however, smaller particles are more bioreactive and can generate free radicals on the surface of the metal oxide [25]. These radicals are cytotoxic and genotoxic, capable of damaging the DNA and skin cells. In addition, these inorganic powders can affect the epidermal layer of the skin and the internal organs of the human body via the respiratory tract [25]. These disadvantages of existing UV filters are still a nuisance to consumers concerned about skin health in the cosmetic market. Therefore, to overcome these problems, human-friendly UV filter materials (bio-based) are being developed as replacements.

Bio-based polymers have shown great potential as alternatives to conventional metallic and organic materials for various applications owing to their biocompatibility, biodegradability, and low carbon emissions [28,29]. Lignocellulosic biomass (LCB), which can be used to produce bio-based polymers, is one of the most promising renewable and abundant carbon-containing resources on Earth [30,31]. Various by-products (or components) can be produced from lignocellulosic biomass. Among them, lignin, silica, and cellulose can be mixed with cosmetic ingredients or industrial polymers, such as polyethylene (PE), polypropylene (PP), and polystyrene (PS), to block or absorb UV rays. Lignin has abundant UV-absorbing functional groups such as conjugated phenols, ketones, quinoid structures, carbon–carbon double bonds, carbonyls, and other chromophores, and effectively absorbs the UVA to UVB range [21,32–37]. Owing to these properties, they were mixed with commercially available sunscreen products to significantly improve their sun protection factor

(SPF) [21]. To encourage the commercial use of lignin, research is underway to improve the color and prove that lignin is harmless to the human body.

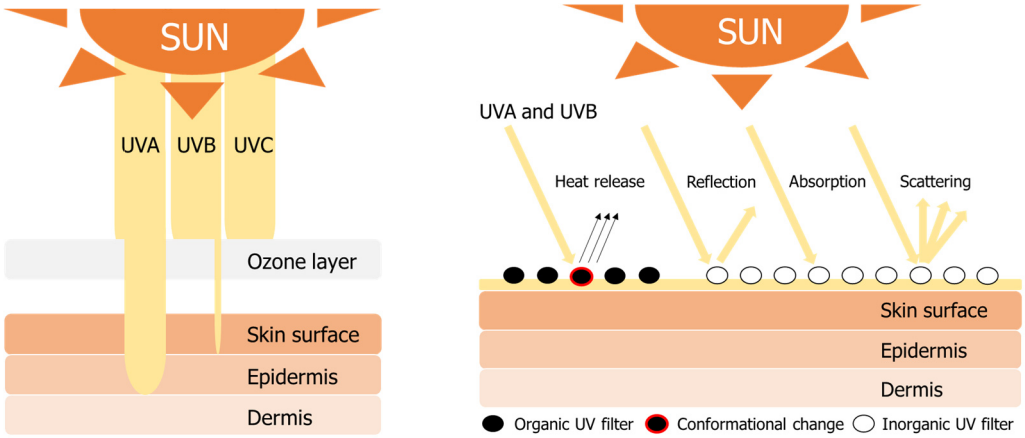

(**a**) (**b**)

Figure 1. UV radiation properties (**a**) penetration into human skin and (**b**) protection mechanisms of organic and inorganic filters.

Table 1. US FDA-approved active ingredients for use in commercial sunscreen products.

Active Ingredient	Concentration Limit (%)	Active Wavelength
Organic		
Aminobenzoic acid (PABA)	15	UVB
Avobenzone	3	UVA2, UVA1
Cinoxate	3	UVB
Dioxybenzone	3	UVB, UVA2
Homosalate	15	UVB
Menthyl anthranilate	5	UVA2
Octocrylene	10	UVB, UVA2
Octyl methoxycinnamate	7.5	UVB
Octyl salicylate	5	UVB
Oxybenzone	6	UVB, UVA2
Padimate O	8	UVB
Phenylbenzimidazole sulfonic acid	4	UVB
Sulisobenzone	10	UVB, UVA2
Trolamine salicylate	12	UVB
Inorganic		
Titanium dioxide	25	UVB, UVA2, UVA1
Zinc oxide	25	UVB, UVA2, UVA1

The enhancement of different inorganic components and their application as UV-blocking materials have been proposed recently [38]. Advanced nanotechnologies such as low-temperature sol-gel and in situ growth of inorganic nanocrystals on the surface of polymer fibers have become more viable over the past decade [39]. Recent research has shown that inorganic components are non-toxic and more stable as UV absorbers and thermal barriers [40]. Lignin has been interpreted as a random, three-dimensional network of natural polymers that is favorable for producing uniform composite structures consisting of inorganic nanoparticles [41]. TiO_2, ZnO, and alumina (Al_2O_3) are the most used inorganic components in UV absorbers [42]. Owing to its extensive band gap (3.36 eV), high electron mobility, and environmentally friendly nature, zinc oxide (ZnO) has gained attention for its utilization as a UV-blocking material [43]. The application of hydrothermal methods in the preparation of one-dimensional ZnO nano- and microstructured materials has provided a rational way to enhance their functions on cotton fabrics with better UV-blocking properties [44]. ZnO is lattice-matched to indium gallium nitride (InGaN) with a

composition of approximately 22%, enhancing the possibility of integrating two different materials [44].

The application of TiO_2 as an inorganic UV-blocking agent has been extensively reviewed owing to its ability to reflect, scatter, and absorb a wide range of UV radiation. Poor dispersibility and strong photocatalytic degradation are the main drawbacks of using TiO_2 directly as a UV-blocking material [45]. Numerous studies have been conducted to reduce the photocatalytic activity of TiO_2. Modification of TiO_2 using various compounds or chemicals has been a well-proposed strategy in recent times for using TiO_2 as a UV-blocking agent. Coating alumina and zeolites with TiO_2 reduces the photocatalytic effect by increasing the band gap at which it is functional to below the UV radiation wavelength of 265 nm [46]. The successive use of lignin recovered from LCB for modifying TiO_2 is highly recommended because of its antioxidant properties and high UV-absorption capacity. Ibrahim et al. worked on synthesizing lignin/TiO_2 and its application as a radical scavenger in sunscreen formulations. In this study, lignin/TiO_2 composites were utilized to suppress the generation of hydroxyl radicals by TiO_2 [47]. Srisasiwimon et al. prepared TiO_2/lignin-based carbon composites using a sol-gel microwave treatment process. In this study, it was observed that carbon from lignin enhanced the UVA irradiation photocatalytic performance of the synthesized composite [48]. Owing to their specific properties, such as high elastic modulus, high thermal and electronic conductivity, and thermal stability, carbon nanotubes (CNTs) have been proposed for use in polymeric materials to ensure UV-shielding [49]. In general, CNTs are classified into two types: (i) single-walled CNTs that consist of one carbonic tube with a diameter of 1–2 nm, and (ii) multi-walled CNTs with multiple concentric tubes. Multi-walled CNTs have high absorption abilities as a UV-blocking material when compared to single-walled CNTs. The improved UV-absorption capacity of CNTs is mainly due to C–C bonding, the narrow shape of carbon atoms, and the availability of free electrons of π-bonds [50]. Nasouri et al. worked on synthesizing CNT fibers with maximum potential as UV-blocking materials. In this study, the maximum UV protection value reached approximately 677 at a thickness of 100 µm [51]. Mahmoudifard and Safi studied the application of single- and multi-walled CNTs as UV-blocking sources for cotton fabric finishing [52]. The SPF is a measure of the minimum erythema dose (MED) and is used as an index to evaluate the ability of a sunscreen to protect the skin from erythema. The SPF factor has been determined using the relationship shown in Equation (1):

$$SPF = \sum_{290}^{400} E_\lambda S_\lambda / \sum_{290}^{400} E_\lambda S_\lambda T_\lambda \quad (1)$$

where E_λ is the CIE (Commission Internationale de l'éclairage or International Commission on Illumination) erythemal spectral effectiveness, S_λ is the solar spectral irradiance, and T_λ is the spectral transmittance of the sample [2].

Hence, in this review, the attributes of biomass-derived UV-shielding compounds are introduced and discussed, including the mechanisms of UV blocking, absorption, preparation methods, chemical and physical properties, and their applications. In particular, various physicochemical properties of lignin that affect UV protection, such as molecular weight, particle size, monolignol ratio, phenol/aliphatic OH content, and junction system, are described. In addition, the types and characteristics of various industrial lignins are summarized to evaluate their potential as sunscreens. Finally, recent research on the applications of fiber and silica as sunscreens is summarized, and the problems and difficulties for successful commercialization are discussed.

2. Effect of Lignin Properties on UV-Shielding Materials

Lignin is a heterogeneous three-dimensional aromatic macromolecule mainly composed of three phenylpropanoid units: *p*-hydroxyphenyl (H), guaiacyl (G), and syringyl (S) linked with β–O–4 (β-aryl ether), α–O–4 (α-aryl ether), 4–O–5 (biphenyl ether), β–5 (phenylcoumaran), β–β (resinol), 5–5 (biphenyl), or β–1 (spirodienones) [53]. These dif-

ferent functional groups and linkages ensure the presence of various chromophores and auxochromes and provide lignin with UV-shielding properties. Currently, the excellent UV absorption ability of lignin has been proven, and studies to accelerate its application to various materials are underway. However, the dark color of lignin makes its use difficult and reduces its potential for added value. The color of native lignin is almost white, but technical lignins such as Kraft lignin, soda lignin, lignosulfonate, and organosolv lignin have a dark color [54–56]. During lignin extraction, various chromophores are formed depending on the solvent or reaction intensity, and the color of the extracted lignin darkens during the extraction or after the extraction, but the exact mechanism is unclear [55].

2.1. Interunit Linkages and Functional Groups of Lignin

Lignin consists of C–C (carbon–carbon) and C–O–C (aryl ether) bonds of three monomers (H, G, and S units) inside the complex structure and contains various functional groups, such as phenolic hydroxyl, methoxyl, and carboxyl. These bonds and functional groups affect the UV-shielding and antioxidant properties of lignin. The chromophore of lignin is an unsaturated group responsible for electron absorption. Currently known chromophores with absorption capacity in the UV region include quinoids, catechols, carbon–carbon bonds, stilbenes, chalcones, conjugated carbonyls with phenolics, and metal complexes [37,57,58]. In addition, auxochromes such as phenolic hydroxyl groups, methoxyl groups, amino groups, –CO, –SH, and $–SCH_3$ are known to greatly affect the UV-shielding performance of lignin [21,33–36,54]. Auxochrome (saturated groups with nonbonding electrons) enhances the UV absorption ability by combining free electron pairs with the aromatic rings of chromophores [59,60]. However, it is impossible to identify the types and roles of all chromophores because of the complex structure of lignin and the challenges in accurate structural analysis [58]. The UV-absorption capacities of lignin compounds with different structures have been studied recently by modifying the lignin into a specific structure or preparing a model compound.

Thermal treatment promotes the demethylation of Kraft lignin by increasing the number of phenolic hydroxyl groups and decreasing aliphatic hydroxyl and methoxyl groups. Widsten et al. converted Kraft lignin into catechol-rich lignin by thermal treatment using softwood and hardwood Kraft black liquor and evaluated its UV transmittance [61]. According to these results, catechol lignin has a better UV-shielding performance than Kraft lignin. This indicates that the phenolic hydroxyl group is more directly related to the UV-shielding performance than the methoxyl group. Phenolic hydroxyl and methoxyl groups are known as major auxochromes and are electron-donating groups. Lin et al. synthesized various lignin model compounds and studied the effect of linkage and functional groups on UV-shielding performance (Figure 2) [62]. The lignin models (LMs) 1–9 contain the typical lignin linkages (β–O–4, β–β, β–5) and various functional groups and structures (phenolic hydroxyl, methoxyl, unsaturated groups, unsaturated groups, and conjugated structures). The results show that the carboxylic acid groups present in the side chain of model lignins are directly involved in improving their SPF. Similar research results were also confirmed by Qian et al.; among five technical lignins, soda, Kraft, sodium lignosulfonate, enzymatic-hydrolyzed lignin, and organosolv lignin with the highest conjugated carbonyl group content had the best UV-absorbing effect [33]. Meanwhile, among the three typical linkages (β–O–4, β–β, and β–5) of lignin, the β–5 linkage showed the highest SPF, considering the structural differences. The UV absorbance is generally increased over the entire UV range (UVA and UVB) as the number of unsaturated groups and conjugated structures is increased.

2.2. Particle Size and Molecular Weight of Lignin

Controlling the particle size of lignin can improve its physicochemical properties, such as structural heterogeneity, dispersibility, specific surface area, and surface permeability, allowing it to be applied in various fields [63,64]. In particular, the nanoparticle size increases the hydrophobic and π–π* stacking interactions in the internal structure of lignin,

and thereby could be modified to improve the antioxidant capacity and UV-absorbing properties [65,66]. The main driving force for the formation of lignin nanoparticles (LNPs) is π–π* interactions rather than electrostatic or van der Waals forces [19,59,63,67]. In addition, nanoparticles improve the dark color of lignin, thus enabling various applications. Attempts have been made to use it as a natural UV-shielding material for personal care products or cosmetics with these characteristics. LNPs are generally produced by the solvent shifting method using chemical solvents, such as tetrahydrofuran (THF), acetone, dioxane, dimethylisosorbide (DMI), isopropylidene glycerol (IPG), or γ-valerolactone (GVL). The lignin dissolved in the selected solvent is then precipitated using an antisolvent (mainly water) to obtain LNPs, which will exhibit different properties depending on the solvent used and the precipitation and drying methods (Table 2).

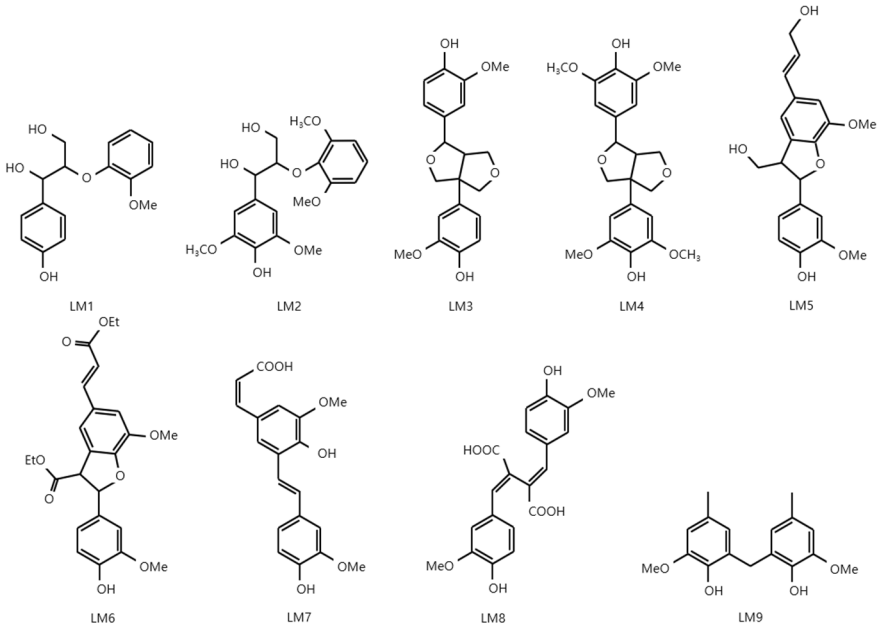

Figure 2. Chemical structures of lignin models.

Table 2. Preparation methods and physical properties of lignin nanoparticles.

Source	Type	Solvent-Shifting	Treatment	Particle Size (nm)	Zeta Potential (mV)	M_w (g/mol)	Ref.
Hardwood	Organosolv	THF (1)	Ultrasonication or magnetic stirring	99	−32.2		[65]
Softwood	Kraft	THF (1)		112	−31.1		
-	Alkali	THF (1)		118	−29.9		
Hardwood	Organosolv	DMI (2)		192	−33.4		
Softwood	Kraft	DMI (2)		89	−29.9		
-	Alkali	DMI (2)		102	−32.5		
Hardwood	Organosolv	IPG (3)		905	−27.3		
Softwood	Kraft	IPG (3)		679	−39.4		
-	Alkali	IPG (3)		780	−28.6		
Hardwood	Organosolv	GVL (4)		101	−31.4		
Softwood	Kraft	GVL (4)		116	−31.8		
-	Alkali	GVL (4)		121	−32.8		
Softwood	Kraft	-	-	440	-	-	[61]
Hardwood	Kraft	-	-	400	-	-	
Softwood	Kraft	Acetone	Agitation	80	-	-	
Hardwood	Kraft	Acetone	Agitation	100	-	-	
Poplar wood	Organosolv	Acetone	Agitation	-	-	2860	[68]
Birch wood	Organosolv	Acetone	Agitation	-	-	4980	
Rice straw	Organosolv	Acetone	Agitation	-	-	2340	
Eucalyptus	Kraft	Ethanol Methanol	Agitation			6428 5143	[69]

Table 2. *Cont.*

Source	Type	Solvent-Shifting	Treatment	Particle Size (nm)	Zeta Potential (mV)	M_w (g/mol)	Ref.
Bamboo	Organosolv	Acetic acid	Agitation	2520	−86.2	3615	[70]
Eucalyptus	Kraft	Acetic acid + Acetylation	-	4150	−68.1	6143	
Elephant grass	Alkali	Acetone	-	55			[71]
	Alkali	Acetylation	-	86			
Bamboo	Organosolv	Acetone	-	-	-	901–5760	[72]
Bamboo	Organosolv	THF [1]	Ultrasonication	205–266			
Corn cob	Alkali	Acetylation	Ultrasonication	100–800			[63]
Pine tree	Alkali	THF [1]	UV radiation	20–200			[55]
-	Kraft	Dioxane	Agitation	100–300			[73]

Note. [1] THF = tetrahydrofuran, [2] DMI = dimethylisosorbide, [3] IPG = Isopropylidene glycerol, [4] GVL = γ-valerolactone.

Solvents that dissolve lignin can affect the morphology and chemical properties of particles by interfering with the non-covalent binding network of the lignin structure [74]. Piccinino et al. prepared and evaluated LNPs using four solvents, namely THF, DMI, IPG, and GVL, using the solvent shift method [65]. Studies have shown that the particle size of lignin varied according to each solvent and grew in the order of IPG > GVL > THF > DMI, and the UV absorbance capacity was inversely proportional to the particle size. This means that the lignin particle size can vary depending on the solvent used, and smaller particle sizes provide better UV-shielding performances. Furthermore, it is related to the distribution of chromophores and auxochromes between the surface and center of the nanoparticles [75]. Li et al. separated acetic acid organosolv lignin extracted from Jiangxi bamboo chips by molecular weight (M_w: 596–2100 g/mol, M_w: 901–5760 g/mol) using acetone [72]. Lignins separated according to their molecular weights were mixed with pure cream to evaluate transmittance. The lower the molecular weight, the better the UV-shielding performance (especially in the UVA region). This enhancement was attributed to the high specific surface area and methoxyl group content. In this study, the molecular weight of lignin decreased with an increase in methoxyl group content between 2.24 to 5.19 mmol/g. Although the methoxyl group is not a chromophore, it is an important electron-donating group that can modify the capacity of the chromophore to absorb long-wavelength UV light [33,76]. Further, the smaller the molecular structure, the higher the absolute value of the zeta potential, and better the dispersion of lignin in the solvent. Eventually, more active points of the UV-shielding effect are exposed, leading to improved UV absorption [70,77]. Another plausible hypothesis is the role of the phenolic and aliphatic hydroxyl groups. According to Li et al., when lignin is decomposed by a specific reaction, the molecular weight decreases, and a new phenolic hydroxyl group is formed as the lignin bond is cleaved [72]. These results explain why low-molecular-weight lignin has more phenolic hydroxyl groups and fewer aliphatic hydroxyl groups than high-molecular-weight lignin. Phenolic hydroxyl groups are known to improve the UV-shielding performance of lignin, while aliphatic hydroxyl groups have been reported to play a role in eliminating the auxochrome component from lignin [61]. Therefore, it is believed that the number of phenolic hydroxyl groups that enhance UV-shielding effects are increased and those of aliphatic hydroxyl groups that remove the auxochrome parts from lignin are decreased in the nanoparticles, consequently improving the sunscreen effect.

Various factors determine the size of LNPs in the solvent shift method. Widsten et al. prepared LNPs from softwood and hardwood Kraft lignin by two precipitation methods: solvent evaporation and dropwise precipitation into an antisolvent [61]. The results showed that the particle size of lignin obtained using the antisolvent method was approximately 4–5 times smaller than that obtained using the solvent evaporation method. Xiong et al. studied the effect of the initial concentration of lignin on the particle size during nanosphere formation by dissolving enzymatically hydrolyzed lignin in THF [67]. According to the

results, the LNP size increased from 327 to 588 nm when the initial concentration of lignin/acetone solution was increased from 0.5 to 2.0 mg/mL. However, in a recent study by Li et al., it was reported that high initial lignin concentration (0.5–2.0 mg/mL) led to the formation of rather small LNPs (205.9–266.4 nm) due to high nucleation density [72]. In other words, a high initial concentration of lignin increases the density and viscosity of the solvent owing to extremely high nucleation, resulting in the formation of small particles. Accordingly, a low initial concentration results in relatively large lignin particles with low density and viscosity owing to low nucleation density. The stirring rate and water-dropping speed during solvent shifting can also affect LNP size. According to Xiong et al., the LNP size decreases with increasing stirring rate and water-dropping speed [67]. However, according to a study by Li et al., the stirring rate and water-dropping speed are not necessarily inversely proportional to LNP size [72]. In principle, as stirring serves to properly mix the aqueous and organic phases, increasing the stirring speed must result in the formation of uniform and small LNPs. However, at excessively high speeds, the balance between the aqueous and organic phases may be lost, adversely affecting the formation of LNPs. In contrast, the pH of the solvent or the treatment temperature did not significantly affect the LNP size, but both did affect the stability [72]. In acidic conditions (pH < 5), aggregation occurred owing to the decrease in the surface charge of the particles, and in alkaline conditions (pH > 11), the particles dissolved. Therefore, it was confirmed that LNP dispersion was most stable in the pH range of 5–11. In addition, high reaction temperature (40 °C) during the formation affects the regularity of LNPs by creating cracks on the lignin surface. The size and shape of LNPs can also be altered by ultrasonication and UV radiation. Wang et al. acetylated corncob alkali lignin using a modified method; it was dissolved in THF and subjected to different ultrasonic intensities (0, 100, and 200 W) [63]. Ultrasonication reduces the size and improves the uniformity of the LNPs. In addition, ultrasound is considered to improve the LNP yield (from 41 to 82.3%), which is believed to play a positive role in nanoparticle formation. Wang et al. dissolved pine alkali lignin in THF and applied 365 nm UV radiation for 200 h. UV radiation decomposed the lignin structure, and as a result, the particle size and molecular weight decreased from 70 to 20 nm and 3000 to 2000 g/mol, respectively [55].

3. Main Factors Affecting the Color of Lignin

The dark color of lignin limits its commercial use. The color of lignin is mainly attributed to its chemical structure and physical properties. Its chemical structure includes phenolic hydroxyl groups, methoxyl groups, lignin-carbohydrate complexes (LCC), condensation and unsaturated structures, conjugation systems, and quinone structures. The physical properties include particle size and morphology, surface area, bulk density, and polydispersity index (PDI). Upon light irradiation, lignin becomes colored when the chromophore absorbs light in the visible range (400–800 nm). This means that the color of lignin can be brightened by removing the chromophore; however, this change is also accompanied by reduced UV absorption ability of lignin. In other words, chemical bleaching improves the color of lignin by brightening it, but concurrently destroys the structure, causing a decrease in its ability to absorb UV rays. Padilha et al. compared UV absorbance spectra before and after bleaching organosolv lignin extracted from cashew apple bagasse [78]. As a result, the bleached lignin was brighter than the unbleached lignin, but its UV absorption capacity decreased in the measurement range (200–800 nm). Strictly speaking, UV absorption capacity is different from the visible light absorption capacity by which the human eye perceives color; however, most chromophores are present in lignin function at both regions. Therefore, reducing the absorption in the visible region and increasing the absorption in the UV region would improve the dark color of lignin while maintaining its UV-shielding performance.

Specular reflection and diffuse reflection refer to the way light is reflected by an object, and the color of an object can appear different depending on the level of specular reflectance. There are two modes for measuring the color of an object: Specular component

included (SCI) mode and specular component excluded (SCE) mode. SCI measurement mode, which includes both specular and diffuse light, is used to measure the true color of an object without the influence of surface conditions, and the SCE measurement mode, which excludes specular light, is used to evaluate the color of an object related to visual perception. The SCI and SCE are used to measure the color of lignin, with three parameters of L*, a*, and b*. Here, L* represents brightness (L* = 100, white; L* = 0, black); +a*, red; –a*, green; +b*, yellow; –b*, blue. The total color difference (ΔE) of each sample was calculated using the following formula:

$$\Delta E = \sqrt{(\Delta L^*)^2 + (\Delta a^*)^2 + (\Delta b^*)^2} \quad (2)$$

where ΔL^*, Δa^*, and Δb^* refer to the differences in color values between the white reference and lignin samples, respectively.

In native wood, lignin is almost colorless but undergoes chemical structural changes caused by high temperature and severe pH conditions during extraction, eventually darkening in color [79–82]. For this reason, most industrial lignins are dark in color because of the various chemical and physical changes that occur during the extraction process. In particular, the phenolic hydroxyl group, an auxochrome of lignin, has an unstable structure and is easily oxidized to quinone, darkening the overall color of lignin, even when present in small amounts [54]. Lee et al. compared the color and properties of three lignins: organosolv lignin (OL), milled wood lignin from *Miscanthus sacchariflorus* (MWL-M), and milled wood lignin from *Pinus densiflora* (MWL-P) (Table 3) [59]. The Δ*E* (white reference) values of OL, MWL-M, and MWL-P were 59.4, 32.7, and 29.4, respectively, and the concentrations of phenolic hydroxyl groups were 3.29, 0.82, and 0.44, respectively. Aliphatic hydroxyl groups in the three lignins presented no significant difference. Milled wood lignin is processed at a mild reaction temperature (~50 °C) to preserve its natural structure while extracting prototype lignin. However, technical lignin (i.e., organosolv lignin) is prepared at high temperatures (125–240 °C) and within a severe pH range (1–5 or 13–14). These severe reaction conditions cause more ether bond cleavage than mild reaction conditions, increasing phenolic hydroxyl groups, which darkens the color [83,84]. Zhang et al. used acetylation to block phenolic hydroxyl groups and enhance the brightness of lignin [85]. Eucalyptus Kraft lignin was acetylated with acetic anhydride, and the color of the lignin was inspected. After acetylation, the L* value of lignin increased by 2.4 times. Qian et al. also reported the color-enhancing effect of acetylation [60]. Wheat alkaline lignin was used to prepare acetylated lignin, and potentiometric titration measurements confirmed that 94% of the phenolic hydroxyl groups in wheat alkaline lignin could be converted into ester groups. In addition, the dark black color of the alkali lignin changed to dark brown after acetylation. The condensation of the lignin structure that occurs during thermal treatments such as pulping or pretreatment darkens the color [67,70]. Zhang et al. compared the methanol-dissolved and undissolved parts of eucalyptus Kraft lignin [70]. Based on the molecular weights of the undissolved and dissolved fractions (5143 and 14,870 g/mol, respectively) and the results of nitrobenzene oxidation (NBO) that showed an obvious decrease in the oxidation yield of the undissolved fraction, it was demonstrated that the undissolved fraction contained more condensed structures. The undissolved fraction contained more quinones or quinone methides, methoxyl groups, diarylmethane structures, and lignin-carbohydrate complexes (LCC) than the dissolved fraction, contributing to the dark color of lignin. Methoxyl groups promote electron transfer in the lignin chromophore, resulting in an auxochrome effect that imparts a dark color to lignin. This also explains why softwood lignin, mainly composed of syringyl units with low methoxyl group content, is brighter than hardwood lignin. Diarylmethanes can readily be dehydrogenated to quinone methide or quinone methide radicals, which in small amounts can contribute significantly to the dark color of lignin [69,86–88]. According to 2D-HSQC NMR (Heteronuclear Single Quantum Coherence Nuclear Magnetic Resonance) data from Zhang et al., xylan structures were identified only in the undissolved portion, indicating that LCC aggregates were

produced under harsh conditions of the pulping process [85]. LCC significantly affects the dark color of lignin compared with phenolic hydroxyl groups [47,78,83,84]. In addition, conjugated double bonds and unsaturated hydrocarbon structures that can be introduced into the lignin side chains in condensation reactions also contribute to the dark color [69].

Table 3. Color properties of lignin depend on the source, type and treatment method.

Source	Type	Further Treatment	SCI [1]			ΔE [2]	ISO [3]	WI [4]	Ref.
			L*	a*	b*	(-)	(%)	(%)	(-)
Hard wood	Organosolv	-	40.6	4.5	4.9	59.4	-	-	[59]
Grass	MWL [5]	-	70.8	7.0	13.8	32.7	-	-	
Softwood	MWL	-	74.6	6.4	14.1	29.4	-	-	
Rice husk	-	-	4.6	21.3	35.5	77.2	-	-	[19]
Rice husk	Organosolv	-	55.1	7.5	15.9	47.8	-	-	
Rice husk	CEL [6]	-	66.8	5.4	15.9	36.8	-	-	
Eucalyptus	Kraft	Acetylation	51.0	8.0	22.7	-	10.4	-	[77]
Eucalyptus	Kraft	Solvent shifting (Pyridine/diethyl ether)	46.5	7.8	17.4	-	8.3	-	
Poplar wood	Organosolv	-	-	-	-	-	-	61.3	[68]
Birch wood	Organosolv	-	-	-	-	-	-	62.2	
Rice straw	Organosolv	-	-	-	-	-	-	45.6	
Bamboo	Organosolv	-	32.4	8.0	21.2	-	5.0	-	[70]
Bamboo	Organosolv	Solvent shifting (acetic acid)	61.7	11.0	23.2	-	17.5	-	
Eucalyptus	Kraft	-	30.6	6.5	18.1	-	3.2	-	
Eucalyptus	Kraft	Acetylation	50.0	8.3	22.5	-	10.4	-	
-	Kraft	Solvent shifting (methanol) undissolved	26.6	5.7	11.6	-	3.0	-	[69]
-	Kraft	Solvent shifting (methanol) dissolved	45.1	10.2	24.1	-	6.1	-	

Note. [1] SCI = specular component included, where L*, a*, and b* refer to the color values of lignin samples (see Equation (2)) [2] ΔE = total color difference value, [3] ISO = Brightness ISO (%), [4] WI = White index ($100 - [(100 - L^*) + a^{*2} + b^{*2}]^{1/2}$), [5] MWL = milled wood lignin, [6] CEL = cellulolytic enzyme lignin.

In addition to differences in chemical structure, physical properties such as particle size, bulk density, and aggregation state significantly influence the color of lignin, and these properties are closely related to each other. For example, small lignin particles increase the absolute value of the zeta potential, increasing the repulsive forces between the particles and eventually reducing the bulk density [77]. A decrease in the bulk density reduces the density of chromophores and macroscopically brightens the color of lignin [70,77]. This implies that the dark color of lignin can be reduced simply by reducing its size. Zhang et al. ground and sorted eucalyptus Kraft lignin by particle size (13.3–143.7 μm), and the bulk density and zeta potential were measured. It was determined that the particle size and bulk density were proportional, whereas the zeta potential was inversely proportional [77]. As expected, the brightness (%ISO) of lignin improved by up to 30% with decreasing particle size (from 143.7 to 13.3 μm) and bulk density (from 0.34 to 0.69 g/cm). In another study by Zhang et al., microspheres were prepared from bamboo lignin using a solvent-shifting method with acetic acid. The prepared acetic acid microsphere lignin was not structurally different from the previous one, but the brightness (ISO%) increased 3.2 times. Meanwhile, the difference in the color of lignin according to physical properties was revealed based on the differences in the drying method [58]. Zhang et al. recovered lignin from the black liquor of eucalyptus Kraft lignin by acid precipitation and compared the colors according to five drying methods: (a) oven drying at 85 °C, (b) air drying under ambient conditions, (c) spray drying, (d) freeze drying at a concentration of 2 g/L, and (e) freeze drying at a concentration of 45 g/L. The drying method affected the aggregation state of dried lignin and resulted in color differences, even though they were structurally identical samples. Despite using the same freeze-drying method, the color difference was markedly dependent on the lignin concentration. Spherical lignin with interparticle spacing was brighter than

oven-dried lignin with dense interparticle spacing. Thus, the particle size, bulk density, and aggregation state of lignin significantly affect lignin color.

4. UV-Shielding Performance of Technical Lignins

Natural lignin has a complex structure and is always linked to carbohydrates (mainly hemicellulose) by covalent bonds, making it practically impossible to be extracted without structural modification [89]. Extraction methods for obtaining unmodified lignin have been developed and are known as MWL and CEL methods [90]. Unlike native lignin, technical lignin refers to lignin obtained as a byproduct of the pulping process using lignocellulosic biomass as the raw material. More than 70 million tons of technical lignin is produced annually, and depending on the chemicals used in the process, it is classified as Kraft lignin, soda lignin, lignosulfonate, and organosolv lignin (Table 4). Technical lignin shows better UV-shielding performance than natural lignin owing to a variety of functional groups and chromophores produced during the severe pulping process. However, the chemical structure, functional groups, and molecular weight of lignin depend on the type of chemical used, which directly determines its optical and dispersion properties [32]. Based on these characteristics, research is being conducted to utilize technical lignin as a UV-shielding agent.

Table 4. Chemical and general properties of technical lignin.

Type (-)	Chemical Use (-)	Solvent (-)	Sulfur Content (%)	Average M_w (g/mol)	Price ($/ton)	Production (per Year)	Ref. (-)
Kraft	Sodium hydroxide and sodium sulfite	Alkali, organic solvents	1.0–3.0	1000–15,000	250–600	70 Mt	[32,90–92]
Lignosulfonate	Aqueous sulfur dioxide	Water	3.5–8.0	1000–50,000	180–500	1 Mt	
Soda	Sodium hydroxide	Alkali	0	1000–3000	200–300	5000–10,000 ton	
Organosolv	Organic solvents	Organic solvents	0	500–5000	300–520	3000 ton	

Qian et al. evaluated the sunscreen performance of five technical lignins: soda lignin, Kraft lignin, organic solvent lignin, enzymatically hydrolyzed lignin, and sodium lignosulfonate (Table 5) [33]. The SPF of the creams mixed with 5% of each technical lignin increased in the following order: organosolv (6.67) > soda (4.01) > Kraft (4.00) > sodium lignosulfonate (3.71) > enzymatically hydrolyzed lignin (3.24). This has been attributed to the higher conjugated carbonyl and methoxyl group content in organosolv lignin than in other lignins; thus, organosolv lignin forms larger and stronger conjugated systems. Accordingly, organosolv lignin had the highest methoxyl group content at 5.19 mmol/g, and enzymatically hydrolyzed lignin had the lowest methoxyl group content at 2.24 mmol/g. By contrast, Lin et al. compared CEL lignin with Kraft lignin and organosolv lignin that were prepared from *Pinus kesiya* (softwood) and *eucalyptus* (grass), respectively, and their UV protection performance was evaluated [62]. As a result, it was found that organosolv lignin and CEL lignin had lower SPF values than Kraft lignin because of their high β–O–4 bond content. In Kraft lignin, more β–O–4 bonds were cleaved because of severe reaction conditions, which may have resulted in an increased content of condensed structures, unsaturated bonds, phenolic hydroxyl groups, and carboxylic acids, which are favorable for UV-shielding performance. Darmawan et al. compared SPF values by mixing three types of lignosulfonate (Ca, Mg, and Na) with tengkawang butter [93]. According to the results, the SPF value decreased in the order of Na-lignosulfonate (7.85) > Mg-lignosulfonate (6.47) > Ca-lignosulfonate (5.68). The SPF value of pure tengkawang butter was 4.04, which improved by 94% (Na-lignosulfonate), 60% (Mg-lignosulfonate), and 40% (Ca-lignosulfonate). Padilha et al. extracted organosolv lignin from cashew apple bagasse using acetic acid and sulfuric acid and evaluated the SPF value by mixing it with pure cream [78]. The SPF values of acetic acid organosolv lignin improved to 1.11, 1.33, and 1.96 as the mixing concentra-

tions of lignin were made at 1%, 2%, and 5%, respectively. Li et al. prepared five types of polyol organosolv lignin, NaOH (soda) lignin, ethylene glycol, glycerol, 1,3-propanediol, and 1,4-butanediol, and compared their UV protection performance [54]. The SPF value of the facial cream mixed with 5% lignin increased in the order of 1,3-propanediol (3.53) > glycerol (3.43) > ethylene glycol (3.37) > 1,4-butanediol (2.54) > soda lignin (2.25). Structural analysis using FTIR and 2D-HSQC NMR revealed more conjugated carbonyl groups in polyol lignin than in soda lignin, which has been proven to be an effective functional group for UV protection. Among the four polyol lignins, there was no difference in the content of chemical structures such as aromatic rings, carbonyl groups, or methoxyl groups derived from the native lignin itself, but there were differences in the contents of LCC and phenolic hydroxyl groups. The contents of LCC and phenolic hydroxyl groups can vary depending on the solvent and reaction severity, which has been identified as the cause of the difference in UV protection performance.

Table 5. Sun protection factors of lignin prepared from various type of lignins.

Source	Type	Chemical	Lignin Conc.	Sun Protection Factor (SPF)				Ref.
(-)	(-)	(-)	(%)	PC [1]	L [2] + PC	SL [3]	L + SL	(-)
-	Soda	-	5	1.0	4.0	18.2	53.7	[33]
	Kraft	-	5		4.0		15.3	
	Organosolv	-	5		6.7		55.7	
	Enzymatic hydrolyzed	-	5		3.2		47.1	
	Na-lignosulfonate	-	5		3.7		22.0	
Eucalyptus	Kraft	-	2	1.0	2.2	16.3	35.4	[62]
	Organosolv	AcOH, formic acid	2		1.7		28.6	
	CEL [4]	-	2		1.3		22.1	
Pinus kesiya	Kraft	-	2		2.3		39.3	
	Organosolv	AcOH, formic acid	2		1.6		24.5	
	CEL [4]	-	2		1.6		24.4	
-	Ca-lignosulfonate	-	1	4.0	5.7	-	-	[93]
-	Mg-lignosulfonate	-	1		6.5		-	
-	Na-lignosulfonate	-	1		7.9		-	
Cashew apple bagasse	Organosolv	AcOH	1	1.0	1.1	21.6	20.1	[78]
	Organosolv	AcOH	2		1.3		29.3	
	Organosolv	AcOH	5		2.0		40.7	
Sugarcane bagasse	Soda	Sodium hydroxide	5	1.1	2.3	12.2	21.9	[54]
	Organosolv	Ethylene glycol	5		3.4		28.1	
	Organosolv	Glycerol	5		3.4		21.0	
	Organosolv	1,3-propanediol	5		3.5		29.3	
	Organosolv	1,4-butanediol	5		2.5		26.5	
Hardwood	Organosolv	-	5	1.1	2.3	8.4	23.6	[59]
Miscanthus sacchariflorus	MWL [5]	-	5		3.2		24.0	
Pinus densiflora	MWL [5]	-	5		2.3		21.3	
Rice husk	CEL [4]	-	5	1.1	2.2	-	-	[19]

Note. [1] PC = pure cream, [2] L = lignin, [3] SL = sunscreen lotion, [4] CEL = cellulolytic enzyme lignin, [5] MWL = milled wood lignin.

Meanwhile, the addition of lignin to chemical-based commercial sunscreens has been shown to significantly improve SPF performance. This fact has been demonstrated in many studies, as shown in Table 5, and may be due to the formation of larger conjugated structures by π–π^* stacking of aromatic rings between lignin and chemical sunscreen active ingredients [33,54]. However, synergistic effects with active inorganic ingredients such as ZnO and TiO_2 have not been reported. Lee et al. prepared CEL and CEL nanoparticles from rice husk, and SPF was determined by mixing aromatic-based (i.e., organic-based) sunscreens and zinc oxide-based sunscreens [19]. As expected, zinc oxide-based sunscreens

did not show synergistic effects similar to chemical sunscreens. This suggests that the structural properties of chemical sunscreens are due to their synergistic effects.

5. Application of Bio-Based Materials as Enhancement Additive for UV-Shielding

Unlike lignin, which is a high-quality UV absorber, some substances are being studied as effective additive; however, they do not have any UV-absorbing properties because of their structural characteristics and physical properties such as porosity, particle size, and large surface area [94–97]. In this review, silica and cellulose fibers are summarized as representative bio-based additives for enhancing UV absorbers.

5.1. UV-Shielding Performance of Biomass-Derived Materials as Enhancement Additives

Silica-based materials are widely used in industrial, biological, pharmaceutical, and electronic applications owing to their properties, such as structure, high surface area, and functionalization [98,99]. Silica is one of the most abundant materials in minerals and plants. It is easy to functionalize (fused quartz, fumed silica, silica gel, or aerogels) and has good biocompatibility, large specific surface area, and large particle size [100,101]. Among the various types of silica-based materials, silica nanoparticles (SiO_2 nanoparticles) have been of interest for various applications. High amounts of active agents (corrosion inhibitors) can be loaded into mesoporous silica owing to their high porosity, which can enhance the basic coating agents or films [102]. In addition, they are considered to possess good absorbability because of their high surface area and mesoporous structure, which are the most important factors for adsorption, regardless of the adsorption being a physical or chemical interaction (covalent or ionic bond) [103,104]. Thus, the advantages of mesoporous silica nanoparticles as fine additives include low reactivity, compatibility in various matrices, low cost, simple surface utilization, and hydrophilic nature [105,106].

Cellulose, which is the most abundant natural resource, is a major component of lignocellulosic biomass. It is composed of a linear chain with repeating units of anhydro-glucose rings linked by β-1,4 glycosidic bonds, which are linkages covalently bonded to C1 of one glucose ring and C4 of the connected ring [95,107]. The monomeric anhydrous-glucose unit consists of three hydroxyl groups that have strong hydrogen bonding with oxygen atoms, which connect the ring molecules in the neighboring chains. These intramolecular and intermolecular hydrogen bonding networks are tightly packed in the crystalline cellulose, stabilizing the linkages; thus, cellulose has a long-chain molecular structure with tough and fibrous properties [108,109]. Cellulose from various sources (wood, plant, algae, animal, etc.), can be utilized for application forms (fiber, microcrystalline cellulose, cellulose nanocrystals, bacterial cellulose particles, etc.) and extraction processes (mechanical, chemical, biological processes, etc.) [95,110–113]. In particular, nanocellulose is the smallest fiber extracted from cellulose with a length of a few micrometers and a diameter of less than 100 nm. In nanoscale particles, the high surface area with numerous hydroxyl groups can contribute to its light weight, low density, and physical properties, such as high stiffness and high tensile strength. Moreover, it also exhibits crystallinity, barrier properties, non-toxicity, and biodegradability; hence, it is considered a promising material for composites, fillers, packaging, and other applications [95,114–116].

Silica and cellulose fibers do not exhibit good light absorption, but because of their properties such as porosity, stability, and hydrophobicity, they can be used as reinforcing agents for UV-absorbing compounds [43,117–120]. UV absorbers can be divided into two types: inorganic and organic compounds. Metal oxides (typically TiO_2, ZnO), representative inorganic UV absorbers, are one of the most studied UV-absorbing materials because of their photocatalytic activity, low cost, and other factors, such as structure, particle size, and crystallinity [121]. The schematic model shows the events that occur when TiO_2 is photoactivated by UV radiation (Figure 3). When metal oxide nanoparticles absorb UV light, they produce conduction band electrons (e^-) and valence band holes (h^+). The electron is donated by an electron acceptor (usually oxygen in the air), whereas the hole migrates to the surface, where an electron from a donor species can combine with the

surface hole, oxidizing the donor species (hydroxyl group). Otherwise, the recombination of electrons and holes occurs in the volume or surface of the particles with the release of heat [122,123]. These metal oxides have been used for many years; however, some problems have emerged in recent studies. Pure ZnO can absorb only the UVA radiation (320–400 nm), and although TiO_2 can absorb both UVA and UVB (290–320 nm), only a part of the UVA can be absorbed [124]. In addition, photochemical reactions can occur on the surfaces of TiO_2 and ZnO during light irradiation, which can cause less effective UV absorption. Moreover, TiO_2 has been reported as a toxic material in vitro, even though there is no evidence of its toxicity on the skin [125]. Therefore, numerous studies have been conducted to enhance their UV absorption and other physical properties, and silica and cellulose fibers have been reported to be effective bulking agents. Modification of TiO_2, by doping or coating with SiO_2, results in a decrease in particle size and an increase in surface area of particles compared with pure TiO_2 modification. In addition, it can decrease the recombination rate of electrons and holes, thereby enhancing the photocatalytic activity of the particles [126,127]. The amorphous phase of SiO_2 bonded with TiO_2 (Ti-O-Si) suppresses the transformation of titania from anatase to rutile, which is an evidence of improved stability [121]. In the case of nanocellulose, Morawski et al. summarized that a 10 wt% TiO_2/nanocellulose composite showed high UV-Vis light absorption, with enhanced water resistivity and thermal and photocatalytic stabilization of cellulosic composites [128]. Also, CNC (cellulose nanocrystal)-ZnO hybrids affected the UV absorption properties (the highest absorbency was 5 wt% in CNC-ZnO loaded PHBV fibers, and 99.95% of UVA and 99.72% of UVB were absorbed); it also improved crystallinity and thermal properties of PHBV composite nanofilms [129].

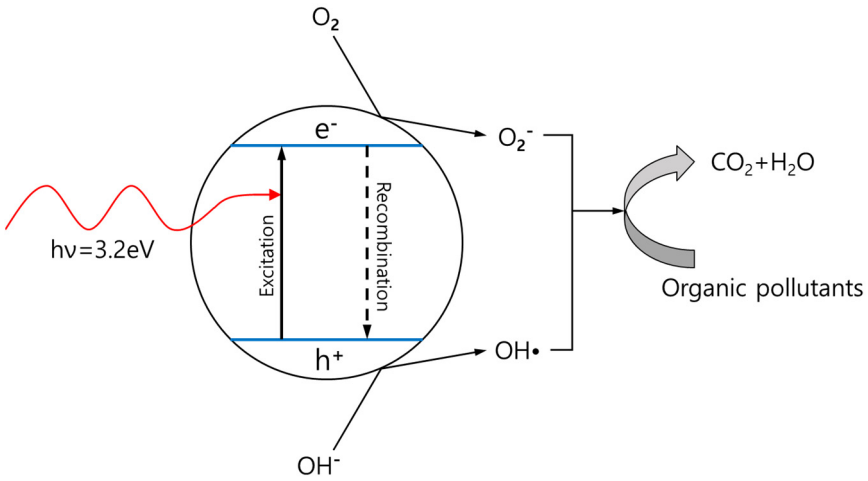

Figure 3. Schematic photoexcitation of metal oxides (TiO_2, ZnO) during absorption of UV radiation.

Organic compounds used as sunscreens are typically classified as UV-absorbing anthranilates, benzophenones, camphors, cinnamates, dibenzoylmethanes, *p*-aminobenzoates, or salicylates. The aromatic groups bonded to the silica compound absorbed UV light because of their delocalized π-electrons. Absorbed UV light is re-emitted as heat or light with lower energy and a longer wavelength or used in photochemical reactions (*cis-trans* or keto-enol isomerization) [130,131]. Aromatic sunscreens mainly absorb UVB radiation, which causes critical skin diseases, and some also absorb UVA radiation [132]. However, in recent studies, sunscreens composed of aromatic UV absorbers have been reported to have significant damaging effects on human cells and DNA [133]. Hence, modifications of aromatic UV absorbers have been carried out using silica- and cellulose-based materials as additives. Amorphous silica is a safe additive (abrasive, anticaking bulking, and opacifying agents) in the cosmetic industry because of its high specific surface area and water absorption capacity; therefore, it is considered an effective enhancement agent [134]. Size-controlled silica can be used to extend the π-bonding of organic UV absorbing agents and

to control the particle size enough to block UV light, and it is small enough for reasonable penetration in the skin, decreasing reactive oxygen species 131]. Similarly, properties such as chemical stability, crystallinity, and degree of hydrogen bonding caused by numerous hydroxyl groups make cellulose nanomaterials perfect additives to enhance aromatic UV absorbers [135,136].

5.2. Extraction of Silica and Nanocellulose from Biomass

Silica-based materials have been used in various industries, most of which have been synthesized from minerals or sand [137,138]. The extraction process requires a high temperature, pressure, or strongly acidic conditions. Thus, it is important to extract silica using efficient processes and cost-effective methods. The synthesis of silica from biomass is easier than its extraction from minerals. Biomass is the most abundant and promising natural resource to replace petrochemical products such as energy sources and chemicals. Rice husk (RH) is an agricultural byproduct that contains 15–28 wt% silica, depending on the climate and origin [139,140]. For economic and environmental reasons, RH is considered a good source of high-quality silica. In 2011, Wang et al. extracted biogenic porous silica nanoparticles with particle sizes of 25–30 nm from rice husks using HCl as a catalyst [141]. The silica nanoparticles from their process showed a porous structure, clustering properties, and low cost. In addition, they reported that it could be converted to a meso/microporous semicrystalline structure by doping with K^+ cations. In 2002, RH ash was produced by calcination at 700 °C for 6 h [142]. Using a simple method of milling and thermal treatment, they generated 95% pure silica powder with a surface area of 81 m^2/g. This method can be considered an environmental-friendly process without the use of any hazardous chemicals. In recent studies, researchers have attempted to fabricate silica for specific applications during the extraction process itself. Wang et al. produced highly photoluminescent carbon-incorporated silica via two-step calcination at 600 °C using acid-treated RH powder [143]. Carbon-incorporated silica has been reported as a promising material for optical, photonic, and biomedical applications because of its non-toxicity and presence of chemically bonded carbon (0.44 wt%).

Three major types of nanocellulose (nanocrystalline, nanofibril, and bacterial) can be extracted from numerous kinds of lignocellulosic biomass by chemical and physical treatments. They can have different particle sizes, crystallinities, and morphologies, depending on the source and extraction method [23]. Yang et al. extracted cellulose nanofibers (CNF) from sugar beet pulp with a diameter of approximately 22 nm [144], and the pulp was pretreated by steam-explosion, bleaching with hydrogen peroxide (H_2O_2), blending, and ultrasonic treatment. The crystallinity index of extracted CNF was 62.3%, and it exhibited good thermal stability. Notably, the extraction efficiency was increased with low energy consumption. In addition, the method used in this study was environmentally friendly compared to other methods that use acid or alkaline catalysts. Dilamian et al. extracted CNF from RH, an agricultural waste [145]. They used chemicals such as sodium chlorite ($NaClO_2$), potassium hydroxide (KOH), and some organic chemicals for pretreatment, followed by ultrasonication. They reported that homogenization and ultrasonication methods could accelerate the fibrillation process, and the diameter of the nanofibers was 6–20 nm. Sofla et al. compared CNC and CNF extracted from sugarcane bagasse [146]. They used a chemical method for CNC and ball milling for CNF. The average particle size of CNC and CNF were 148 and 240 nm, respectively, with the length of CNF being approximately 10 μm. The aspect ratio of the CNF contributed to thermal stability, whereas there was no enhancement in the thermal stability of CNC value.

6. Application of Biomass-Derived UV-Shielding Materials

6.1. Applications of Lignin as a UV-Absorbing Agent

UV absorption capacity is a well-known functionality of lignin because of its chromophore structure [147]. Lignin contains various conjugated groups, such as conjugated ketones, quinoid structures, phenolics, and intramolecular hydrogen bonds [21,32–36,85].

As conjugated chemical moieties of materials can function as UV chromophores, lignin has been investigated in UV-absorbing applications [34,148]. In addition, phenolic hydroxyl groups in the lignin structure positively affect free radical scavenging activity and promote antioxidant properties [38,149–151]. Regarding the specific absorption range of each conjugated group in lignin, it was suggested that conjugated ketones absorb radiation in the range of 250–300 nm, quinoid in the range of 375–425 nm, and conjugated phenolics in the range of 475–600 nm due to their conjugated length [2,152]. However, it should be noted that slight modifications to the chromophore structure can cause a shift in the absorption spectrum. In addition to the structure of lignin, a photochemical reaction of lignin (i.e., yellowing) via UV irradiation causes the formation of other chromophore structures, which is also beneficial for UV-absorbing applications [151,153]. This section summarizes the applications of lignin as a UV absorber. Examples of lignin applications, including sunscreens, composites, and surfactants with specific capabilities, are summarized in Table 6.

Table 6. Various valorization strategies of plant-based materials with their modification mechanisms, properties, and UV protection aspects.

Types of Materials	Modifications	Concentrations	SPF	Other Properties	Applications	Ref.
Organic acid lignin	Acetic acid/ hydrogen peroxide/HCl	5 wt%	5	Antioxidant activity	Sunscreen	[149]
Alkali lignin	Grafting the benzophenone	10 wt%	56	Antioxidant activity	Sunscreen	[150]
Sulfonated alkali lignin	Grafted on TiO_2	20 wt%	48	N/A	Sunscreen	[154]
Kraft, alkali lignin	Fabricating the ZnO particles	20 wt%	10	Antioxidant activity Antimicrobial activity	Sunscreen	[38]
Soda, organosolv lignin	Compose with ZnO nanoparticles	5 wt%	13	Photostability	Sunscreen	[155]
Kraft lignin	Synergistic effect with commercial products	8 wt%	75	Decolorization	Sunscreen	[87]
Organosolv lignin	Synergistic effect with commercial products	10 wt%	92	Photostability	Sunscreen	[33]
Alkali lignin	Synergistic effect with commercial products	10 wt%	50	Photostability	Sunscreen	[21]
CEL, organosolv lignin	Synergistic effect with commercial products	5 wt%	30	Decolorization	Sunscreen	[19]
Kraft lignin	Solvent blending	5 wt%	Good	Photostability	Composites (PVC)	[156]
Organosolv lignin	Fractionation, solvent casting	1 wt%	0.8% [a]	Plasticizer effect Antioxidant activity	Composites (PMMA)	[157]
Soda lignin	Grafting the oleic acids, melt-blend	10 wt%	1% [a]	Enhanced tensile properties	Composites (PBAT)	[158]
Alkali lignin	Solvent blending	50 wt%	50 [b]	Electrospinning Antimicrobial activity	Composites (PVA)	[159]
Alkali lignin	Etherification, solvent casting	10 wt%	50 [b]	Wettability Moisture adsorption Swelling efficiency	Composites (PVA)	[160]
Organosolv lignin	TiO_2 decoration, blade-casting	5 wt%	10% [a]	Thermal stability Enhanced modulus	Composites (PPC)	[161]
Softwood Kraft lignin	Propargylation, solvent casting	2 wt%	100	Thermal stability	Composites (cellulose)	[34]
Alkaline and softwood Kraft lignin	Acetylation, solvent casting	4 wt%	41	Decolorization Surface hydrophobicity Thermal stability	Composites (cellulose)	[35]
Kraft lignin	Solvent casting	10 wt%	53.6% [a]	Enhanced tensile strength, Surface hydrophobicity Water vapor permeabilities Antioxidant activity Non-cytotoxic activity	Composites (gellan gum, cellulose)	[162]
Kraft lignin	Acetylation, solvent casting	10 wt%	2.5% [a]	Barrier property, Solubility parameter analysis Enhanced tensile properties	Composites (PLA)	[163]
Enzymatic and milled lignin	Knife casting	20 wt%	0% [a]	Flame retardant grade Moisture/gas transmittance	Composites (MMT)	[164]

Table 6. *Cont.*

Types of Materials	Modifications	Concentrations	SPF	Other Properties	Applications	Ref.
Enzymatic lignin	Ozone oxidation	N/A	Excellent	Antioxidant activity	Surfactant	[151]
Enzymatic hydrolysis lignin	Grafting alkyl polyglucoside	2 wt%	Superior	N/A	Surfactant	[165]
cellulose nanocrystal	Grafting aldehyde and *p*-aminobenzoic acid	10 wt%	0% [a]	Transparency Enhanced tensile strength	Composites (PVA)	[136]
Cellulose acetoacetates	Biginelli reaction with urea and vanillin	N/A	0% [a]	Transparency	Cellulose film	[166]
TEMPO-oxidized cellulose	Grafting curcumin	33 wt%	23% [a]	Vapor barrier properties	Composites (chitosan)	[167]
Cellulose nanocrystal	Grafting phenolic ester	20 wt%	0% [a]	Transparency Enhanced tensile properties	Composites (PVA)	[168]
Cellulose microfiber	Aldolization	N/A	Strong	Transparency Wettability	Composites (PVA)	[169]
Mesoporous silica nanoparticle	N/A	N/A	19	N/A	N/A	[142]
Silica vesicle	Encapsulation of MBBT	37.5 wt%	100	Water dispersibility	Sunscreen	[170]
Mesoporous silica	Encapsulation of octyl methoxycinnamate	4 wt%	13	N/A	Sunscreen	[171]
Mesoporous silica	Compose with titania and tannin	5 wt%	42	N/A	Sunscreen	[172]
Calcium silicate	N/A	5 wt%	38	Less white residue	Sunscreen	[173]
Fumed silica nanoparticles	N/A	0.1 wt%	N/A	Decreasing in aging factor	Composites (bitumen)	[174]

[a] Transmittance, [b] UPF: Ultraviolet protection factor.

The UV absorption property of lignin allows its application in sun protection. With the simple addition of lignin (5 wt%) to moisture lotion, the sun protection factor (SPF) of the moisture cream was increased to 5 [149]. To maximize the UV-absorbing properties of lignin, different strategies, such as structure modification and self-assembly of lignin, strategy using lignin-metal oxide composites, and infusion with commercial sunscreen products, have been studied. Wu et al. introduced a benzophenone moiety into the lignin structure; the SPF of sunscreen with 10 wt% lignin reached 23, while that with unmodified lignin was only 8 [150]. In the same study, by achieving a self-assembled structure of modified lignin, the SPF of benzophenone-activated lignin was further enhanced to 56.

Lignin is also useful as a stabilizing and fabricating agent. Metal oxides such as TiO_2 and ZnO, which are one of the most common substances for inorganic UV fillers, have been introduced to compose lignin [38,154,155]. Kaur et al. utilized lignin as a capping and stabilizing agent for ZnO particles to fabricate ZnO nanocomposites via a one-pot reaction [38]. Lignin-derived ZnO nanocomposites, commercial ZnO nanoparticles, and native lignin were included in sunscreen at a concentration of 20 wt%. Sunscreen with lignin-derived ZnO nanocomposites had higher SPF values (10) than those with native lignin and commercial ZnO (2 and 4, respectively). Gutiérrez-Hernández et al. also demonstrated the use of lignin with ZnO for sunscreen applications [155]. Soda and organosolv lignins were modified with different concentrations (18% and 27%) of formaldehyde for fabricating them to nanoparticles with ZnO. Sunscreens were prepared using different concentrations of LNPs in a commercial moisture lotion. The SPF value of sunscreen with organosolv LNPs was similar to that of commercial ZnLNP, whereas that with the same concentration of soda LNPs showed lower values. Furthermore, the SPF of sunscreen containing both commercial ZnLNP and organosolv LNP was almost 1.5 times higher than that of sunscreens with the same concentration of a single nanoparticle. The synergistic effect of lignin with commercial UV-absorbing products on UV protection ability has been reported in other previous studies [19,21,33,87]. Qian et al. increased the SPF of commercial sunscreen from 15 to 30 by adding 2 wt% of alkali lignin and further improved it to 50 with 10 wt% of the lignin [35]. The team also investigated various technical lignins for use in commercial sunscreens [34]. Among several tested lignins, relatively

hydrophobic lignins (e.g., oligosolv lignin) showed a better synergistic effect on active materials in commercial sunscreen than hydrophilic ones (e.g., sodium lignosulfonate). These synergistic effects can be explained based on the π–π stacking between commercial sunscreen actives and lignins via the formation of conjugated chromophores.

The conjugated groups in lignin help to absorb UV irradiation, but they also absorb a certain portion of the lower end of the visible spectrum, inducing a symbolic dark-brown color, which is a major challenge for lignin-containing sunscreens. To overcome this obstacle, the decolorization of lignin by fractionation followed by acetylation and application of mild extraction conditions has been studied [19,87]. Zhang et al. whitened Kraft lignin by methanol fractionation, followed by acetylation [87]. After the two-step treatment, the brightness of the lignin was increased by 313.5%. The whitened lignins showed great synergistic effects with commercial sunscreen, increasing the SPF of sunscreen from 15 to 75.

The UV absorption of lignin is also featured in applications of lignin-based composite materials. Various polymers such as polyvinyl acetate (PVC), poly(methyl methacrylate) (PMMA), poly(butylene adipate-co-terephthalate) (PBAT), poly(vinyl alcohol) (PVA), poly(propylene carbonate) (PPC), and cellulose were combined with lignin to utilize its UV absorption and antioxidant properties [34,35,156–162]. Avelino et al. incorporated the ethanol fractionated organosolv lignin into a PMMA film by solvent casting at different concentrations (0%, 0.25%, 0.5%, 1.0%, 2.5%, and 5.0%) [158]. The transmittance of neat PMMA film was 45% and 62% in the UVB and UVA ranges, respectively. By introducing 1 wt% of lignin into the film, it decreased by 0.8% and 3.4%, respectively. Notably, the ethanol-soluble fraction of lignin exhibited a plasticizer effect, decreasing the glass transition temperature of the PMMA/lignin composite. Additionally, the fractionation of lignin caused an increase in the transparency of the treated film from 26% to 79% compared with that by non-treated lignin/PMMA film. One of the challenges in creating composite materials is the homogeneous mixing of different elements. To facilitate compatibility between lignin and the polymer matrix, covalent bonding, acetylation, aqueous alkaline suspension, etherification by citric acid, and esterification (grafting) were considered [34,158,160,161,163]. Xing et al. reported the grafting of oleic acids onto the lignin surface to facilitate high compatibility with PBAT [158]. The composite was prepared by the extrusion method, which is cost-effective but makes it difficult to achieve homogeneous mixing compared with solvent casting. Compared with the non-grafted lignin composites, significant increment in elongation at break increased from 418% to 679% while maintaining a similar tensile strength. In addition, clay minerals (montmorillonite, MMT) were combined with lignin at a molar ratio of 8:2 to fabricate a non-flammable film (lignoclaist) with excellent UV protection and moisture/gas permeability [164]. With the thin layer of films (26 μm), the transmittance of the UVB and UVA was 0% and 1.2%, while transparency over visible light was 56%. In addition to the aforementioned applications, lignin can also be fabricated as a surfactant. By ozone oxidation of lignin and grafting to polyethylene glycol (PEG) or sulfomethylation, lignin shows surfactant ability and preserves unique properties such as UV absorption, antioxidant, and antibacterial properties [151,165].

6.2. Applications of Cellulose as a UV-Absorbing Agent

Several studies have reported the application of cellulose as a UV-absorbing agent. Although cellulose is not an effective UV-absorbing agent, it shows effective UV absorption after adopting UV-absorbing conjugated moieties to its structure via chemical modification methods. Sirviö et al. modified CNCs by introducing aldehyde groups and *p*-aminobenzoic acid and produced a composite film with PVA [136]. The composite film with 10 wt% of modified CNC completely screened UVA and UVB rays and maintained more than 80% transparency over the entire visible light region. The addition of modified CNC also improved the mechanical strength of PVA. Typically, these films are used for packaging applications; therefore, their tensile strength is an important characteristic. Compared with the tensile strength and modulus of neat PVA, those of nanocomposite films were enhanced

up to 33% and 77%, respectively, with the above-mentioned UV absorption. Yuan et al. modified the cellulose structure via the Biginelli reaction between urea and vanillin [166]. This modified cellulose was fabricated into a film with a thickness of 100 µm, resulting in a complete screen of UVA and UVB with 80% transparency in the visible light spectrum. The grafting of curcumin into CNFs has also been reported by Zhang et al. The authors reported that curcumin-grafted cellulose exhibited antibacterial, antioxidant, and UV-absorption properties [167]. Specifically, curcumin-grafted TEMPO (2, 2, 6, 6-tetramethylpiperidine-1-oxyl)-oxidized CNFs were introduced into the chitosan film. The UV absorbing ability (at 400 nm) of the film composed of 33 wt% modified cellulose was 77% higher than that of pure chitosan film. Similarly, CNCs grafted with a phenolic diester (DEF) have been compounded with PVA [168]. The PVA film with 20 wt% of the modified CNCs showed complete UV protection with high transparency (70–90%) in the visible range. In addition, the tensile strength and modulus of the CNC-DEF-loaded PVA composite films were up to 91 and 150% higher than these properties of the neat PVA film.

Feng et al. formed cellulose microfibers (CMFs) from rice straw via delignification using a 9 wt% NaOH solution, followed by a low-temperature phase transition [169]. The acquired CMF was further treated with $NaIO_4$ to introduce aldehyde for aldolization with the PVA matrix during its compounding. The optimized CMF/PVA composites showed an increased tensile strength of 38 MPa compared with that of neat PVA (26 MPa). Also, 70 µm thick films showed strong absorption in the UV range while retaining 80% transparency to visible light. The possible UV absorption mechanism of this composite from the remaining lignin building blocks in CMF is also discussed in this article. Detailed examples are presented in Table 6.

6.3. Applications of Silica as a UV-Blocking Agent

Some nanoscale particles, such as TiO_2 and ZnO, have been applied as predominant materials for reflecting and scattering UV light. However, to increase biocompatibility and alleviate the environmental and health concerns of these metal oxides in sun protection products, silica (Si), which can be obtained from biomasses such as corn cob, rice husk, sugarcane bagasse, and husk, has been studied as an alternative material [170–173]. Various strategies for enhancing the UV-blocking ability of Si and their applications are listed in Table 6. Knežević et al. fabricated tetraethoxysilane (TEOS) into mesoporous silica nanoparticles (MSNs) for the application of SiO_2 in sunblock products. Periodic mesoporous organosilica nanoparticles (PMOs), which have a structure similar to MSNs, were also fabricated by bridging Si with ethane (PMOBTE) or benzene (PMOBTB) for the same application [138]. MSNs showed the lowest SPF value (1) owing to their small size, which is ineffective for scattering UVB and UVA. PMOBTE and PMOBTB, with average diameters of 541 and 357 nm, respectively, showed SPF values of 9 and 19, respectively. This result supports the UV protection mechanism of these PMOs based on their chemical structures. In addition, the impact of nanoparticle size on the UV protection performance was evaluated using PMOBTB with a smaller diameter. PMOBTB with a diameter of 114 nm showed an SPF of 10, which was lower than that at 357 nm (19). Silica has been applied as a carrier of organic UV absorbers and is composed of conventional inorganic materials for blocking UV in cosmetic products [174–176]. Methylene-bisbenzotriazolyl tetramethylbutylphenol (MBBT) is a good organic-based UV-absorbing material, and its hydrophobic nature is highly concentrated in cosmetics [177]. Zhang et al. fabricated an MBBT-embedded silica vesicle structure with an SPF value of 100 [174]. In addition, encapsulation with silica particles increased water dispersibility without the aid of dispersing agents.

One of the main drawbacks of using conventional inorganic particles (i.e., TiO_2 and ZnO) for sunblock cosmetics is the whitening effect, in which the scattering of light extends to the visible ray [178,179]. To solve this issue, calcium silicate (Ca_2SiO_4) salt found in soils was used to fabricate sunblocks [180]. The results showed that using 5 wt% Ca_2SiO_4 helped to achieve an SPF of 38, which is better than using the same amount of ZnO (25) or TiO_2 (48). In addition, sunblock with less white residue can be achieved owing to the

low refractive index of Ca_2SiO_4 (1.6), in which conventional inorganic fillers have values greater than 2.0. Silica has also been used as a UV-blocking agent in bitumen, which is the main component of asphalt [181]. UV exposure to bitumen aggravated the stiffness level of the samples, which reduced their aging. The index of viscosity aging significantly decreased by introducing fumed silica nanoparticles with a content of 0.1 wt%.

In summary, biomass components have been examined as UV-blocking agents for various applications. Lignin shows excellent absorption capability over a broad UV range without any further modification because of its conjugated structure. However, the unique brownish color of lignin limits its application, particularly in cosmetic products. The intrinsic structure of cellulose is not ideal for UV absorption; therefore, chemical modification is commonly performed. Thus, cellulose can be utilized as the main ingredient for UV-screening films or bio-based anti-UV additives for polymer composites while showing great transparency in visible light. Silica has also been utilized as an active material for UV protection. Owing to its lower refractive index than conventional inorganic UV fillers, silica can achieve less white stain with decent UV-blocking properties.

7. Conclusions

In this review, the various effects and mechanisms of biomass-derived materials for UV-shielding are discussed. Lignocellulosic biomass-derived materials have the potential to be used as UV-shielding agents to protect polymers and human skin from UV rays. In this study, various topics such as the chemical structure and functional groups between lignin units, the main factors affecting the color of lignin, and the UV-shielding effect of various materials such as silica, nanocellulose, and fibers were reviewed. However, the valorization of biomass-derived materials is still a big challenge, and commercialization will not be easy unless price competitiveness is overcome. However, the society is currently moving towards the goal of carbon neutrality and sustainable development, greatly realizing that the environment must take precedence over material values. In particular, chemical structures and functional groups between lignin units, major factors affecting the color of lignin, and UV shielding effects of various materials such as silica, nanocellulose, and fibers were reviewed. For example, the lignin-based UV filter is a natural material that can overcome fatal disadvantages such as irritation, allergic contact reaction, cytotoxicity, and genotoxicity of existing organic and inorganic UV filters. Various chromophores, auxochrome, and functional groups present in lignin not only directly show UV shielding properties, but also greatly improve UV shielding properties that can be expected due to synergistic effects when mixed with existing sunscreen cream. Unlike lignin, silica and fiber have low UV-shielding effects, but can act as reinforcing agents for UV-shielding compounds due to their porosity, stability, and hydrophobicity. As reviewed in this paper, lignocellulosic biomass-derived materials have the potential to be used as UV-shielding agents to protect polymers and human skin from UV rays. Although there are major obstacles to be overcome in price competition with existing UV-shielding agents, the recent change in consumer awareness is predicting a positive sign. As the quality of life improves, more and more consumers prefer human-friendly and eco-friendly products, even considering the high cost. In addition, a social atmosphere that considers not only the product's intrinsic value but also social and environmental values will clearly indicate the direction in which we should move forward.

Author Contributions: Conceptualization, T.H.K. (Tae Hyun Kim) and C.G.Y.; writing—original draft preparation, T.H.K. (Tae Hoon Kim), S.H.P., S.L. and A.V.S.L.S.B.; writing—review and editing, S.H.P., S.L., A.V.S.L.S.B. and Y.S.L. All authors have read and agreed to the published version of the manuscript.

Funding: This work was supported by the Materials, Components & Equipment Research Program funded by Gyeonggi-do (No. AICT-01-T1) and R&D program of Korea Evaluation Institute of Industrial Technology (KEIT) grant funded by the Ministry of Trade, Industry &Energy (MOTIE), Korea (No. RS-2022-00156062).

Data Availability Statement: No new data were created or analyzed in this study. Data sharing is not applicable to this article.

Acknowledgments: We are deeply grateful to Jeong Pyo Hong and Dae Il Hwang of Samwon Industrial Co., Ltd., for their kind support.

Conflicts of Interest: The authors declare no conflict of interest.

References

1. Nichols, J.A.; Katiyar, S.K. Skin photoprotection by natural polyphenols anti-inflammatory: Antioxidant and DNA repair mechanisms. *Arch. Dermatol. Res.* **2010**, *302*, 71–83. [CrossRef]
2. Sadeghifar, H.; Ragauskas, A. Lignin as a UV light blocker—A review. *Polymers* **2020**, *12*, 1134. [CrossRef]
3. Hattori, H.; Ide, Y.; Sano, T. Microporous titanate nanofibers for highly efficient UV-protective transparent coating. *J. Mater. Chem. A* **2014**, *2*, 16381–16388. [CrossRef]
4. Miao, Y.; Tang, Z.; Zhang, Q.; Reheman, A.; Xiao, H.; Zhang, M.; Liu, K.; Huang, L.; Chen, L.; Wu, H. Biocompatible Lignin-Containing Hydrogels with Self-Adhesion, Conductivity, UV Shielding, and Antioxidant Activity as Wearable Sensors. *ACS Appl. Polym. Mater.* **2022**, *4*, 1448–1456. [CrossRef]
5. Xiong, F.; Wu, Y.; Li, G.; Han, Y.; Chu, F. Transparent Nanocomposite Films of Lignin Nanospheres and Poly(vinyl alcohol) for UV-Absorbing. *Ind. Eng. Chem. Res.* **2018**, *57*, 1207–1212. [CrossRef]
6. Andrady, A.L.; Hamid, S.H.; Hu, X.; Torikai, A. Effects of increased solar ultraviolet radiation on materials. *J. Photochem. Photobiol. B Biol.* **1998**, *46*, 96–103. [CrossRef] [PubMed]
7. Dahms, H.U.; Dobretsov, S.; Lee, J.S. Effects of UV radiation on marine ectotherms in polar regions. *Comp. Biochem. Physiol. Part C Toxicol. Pharmacol.* **2011**, *153*, 363–371. [CrossRef]
8. Madronich, S.; McKenzie, R.L.; Björn, L.O.; Caldwell, M.M. Changes in biologically active ultraviolet radiation reaching the Earth's surface. *J. Photochem. Photobiol. B Biol.* **1998**, *46*, 5–19. [CrossRef]
9. Mandi, S.S. UV Radiation-Induced Damage at Molecular Level. In *Natural UV Radiation in Enhancing Survival Value and Quality of Plants*; Springer: New Delhi, India, 2016; pp. 45–71.
10. Melnikova, V.O.; Ananthaswamy, H.N. Cellular and molecular events leading to the development of skin cancer. *Mutat. Res. Fundam. Mol. Mech. Mutagen.* **2005**, *571*, 91–106. [CrossRef] [PubMed]
11. Crawford, J.C. 2(2-hydroxyphenyl)2H-benzotriazole ultraviolet stabilizers. *Prog. Polym. Sci.* **1999**, *24*, 7–43. [CrossRef]
12. Schaller, C.; Rogez, D.; Braig, A. Hydroxyphenyl-s-triazines: Advanced multipurpose UV-absorbers for coatings. *J. Coat. Technol. Res.* **2008**, *5*, 25–31. [CrossRef]
13. Denisov, E.T. The role and reactions of nitroxyl radicals in hindered piperidine light stabilisation. *Polym. Degrad. Stab.* **1991**, *34*, 325–332. [CrossRef]
14. Klampfl, C.W.; Himmelsbach, M. Advances in the determination of hindered amine light stabilizers—A review. *Anal. Chim. Acta* **2016**, *933*, 10–22. [CrossRef]
15. Geoffrey, K.; Mwangi, A.N.; Maru, S.M. Sunscreen products: Rationale for use, formulation development and regulatory considerations. *Saudi Pharm. J.* **2019**, *27*, 1009–1018. [CrossRef]
16. Shaath, N.A. Ultraviolet filters. *Photochem. Photobiol. Sci.* **2010**, *9*, 464–469. [CrossRef] [PubMed]
17. Manaia, E.B.; Kaminski, R.C.K.; Corrêa, M.A.; Chiavacci, L.A. Inorganic UV filters. *Braz. J. Pharm. Sci.* **2013**, *49*, 201–209. [CrossRef]
18. Geisler, A.N.; Austin, E.; Nguyen, J.; Hamzavi, I.; Jagdeo, J.; Lim, H.W. Visible light. Part II: Photoprotection against visible and ultraviolet light. *J. Am. Acad. Dermatol.* **2021**, *84*, 1233–1244. [CrossRef]
19. Lee, S.C.; Yoo, E.; Lee, S.H.; Won, K. Preparation and application of light-colored lignin nanoparticles for broad-spectrum sunscreens. *Polymers* **2020**, *12*, 699. [CrossRef] [PubMed]
20. U.S. Food and Drug Administration: Part 352-Sunscreen Drug Products for Over-the-Counter Human Use. Available online: https://www.accessdata.fda.gov/scripts/cdrh/cfdocs/cfcfr/CFRSearch.cfm?fr=352.10 (accessed on 6 January 2023).
21. Qian, Y.; Qiu, X.; Zhu, S. Lignin: A nature-inspired sun blocker for broad-spectrum sunscreens. *Green Chem.* **2015**, *17*, 320–324. [CrossRef]
22. Butt, S.T.; Christensen, T. Toxicity and phototoxicity of chemical sun filters. *Radiat. Prot. Dosim.* **2000**, *91*, 283–286. [CrossRef]
23. Jansen, R.; Osterwalder, U.; Wang, S.Q.; Burnett, M.; Lim, H.W. Photoprotection: Part II. Sunscreen: Development, efficacy, and controversies. *J. Am. Acad. Dermatol.* **2013**, *69*, 867.e1–867.e14. [CrossRef] [PubMed]
24. Lautenschlager, S.; Wulf, H.C.; Pittelkow, M.R. Photoprotection. *Lancet* **2007**, *370*, 528–537. [CrossRef]
25. Ruszkiewicz, J.A.; Pinkas, A.; Ferrer, B.; Peres, T.V.; Tsatsakis, A.; Aschner, M. Neurotoxic effect of active ingredients in sunscreen products, a contemporary review. *Toxicol. Rep.* **2017**, *4*, 245–259. [CrossRef] [PubMed]
26. Kajta, M.; Wójtowicz, A.K. Impact of endocrine-disrupting chemicals on neural development and the onset of neurological disorders. *Curr. Pharmacol. Rep.* **2013**, *65*, 1632–1639. [CrossRef] [PubMed]
27. Lowe, N.J. An overview of ultraviolet radiation, sunscreens, and photo-induced dermatoses. *Dermatol. Clin.* **2006**, *24*, 9–17. [CrossRef] [PubMed]

28. Ramakrishna, S.; Mayer, J.; Wintermantel, E.; Leong, K.W. Biomedical applications of polymer-composite materials: A review. *Compos. Sci. Technol.* **2001**, *61*, 1189–1224. [CrossRef]
29. Thakur, V.K.; Thakur, M.K.; Gupta, R.K. Raw natural fiber–based polymer composites. *Int. J. Polym. Anal. Charact.* **2014**, *19*, 256–271. [CrossRef]
30. Doherty, W.O.; Mousavioun, P.; Fellows, C.M. Value-adding to cellulosic ethanol: Lignin polymers. *Ind. Crops Prod.* **2011**, *33*, 259–276. [CrossRef]
31. Bruijnincx, P.C.; Weckhuysen, B.M. Lignin up for break-down. *Nat. Chem.* **2014**, *6*, 1035–1036. [CrossRef]
32. Tran, M.H.; Phan, D.P.; Lee, E.Y. Review on lignin modifications toward natural UV protection ingredient for lignin-based sunscreens. *Green Chem.* **2021**, *23*, 4633–4646. [CrossRef]
33. Qian, Y.; Qiu, X.; Zhu, S. Sunscreen performance of lignin from different technical resources and their general synergistic effect with synthetic sunscreens. *ACS Sustain. Chem. Eng.* **2016**, *4*, 4029–4035. [CrossRef]
34. Sadeghifar, H.; Venditti, R.; Jur, J.; Gorga, R.E.; Pawlak, J.J. Cellulose-lignin biodegradable and flexible UV protection film. *ACS Sustain. Chem. Eng.* **2017**, *5*, 625–631. [CrossRef]
35. Parit, M.; Saha, P.; Davis, V.A.; Jiang, Z. Transparent and homogenous cellulose nanocrystal/lignin UV-protection films. *ACS Omega* **2018**, *3*, 10679–10691. [CrossRef]
36. Ajao, O.; Jeaidi, J.; Benali, M.; Restrepo, A.M.; El Mehdi, N.; Boumghar, Y. Quantification and variability analysis of lignin optical properties for colour-dependent industrial applications. *Molecules* **2018**, *23*, 377. [CrossRef] [PubMed]
37. Zhang, Y.; Naebe, M. Lignin: A review on structure, properties, and applications as a light-colored UV absorber. *ACS Sustain. Chem. Eng.* **2021**, *9*, 1427–1442. [CrossRef]
38. Kaur, R.; Thakur, N.S.; Chandna, D.; Bhaumik, J. Development of agri-biomass based lignin derived zinc oxide nanocomposites as promising UV protectant-cum-antimicrobial agents. *J. Mater. Chem. B* **2020**, *8*, 260–269. [CrossRef] [PubMed]
39. Abidi, N.; Hequet, E.; Tarimala, S.; Dai, L.L. Cotton Fabric Surface Modification for Improved UV Radiation Protection Using Sol-Gel Process. *J. Appl. Polym. Sci.* **2007**, *104*, 111–117. [CrossRef]
40. Wang, M.; Zhang, M.; Pang, L.; Yang, C.; Zhang, Y.; Hu, J.; Wu, G. Fabrication of highly durable polysiloxane-zinc oxide (ZnO) coated polyethylene terephthalate (PET) fabric with improved ultraviolet resistance, hydrophobicity, and thermal resistance. *J. Colloid Interface Sci.* **2019**, *537*, 91–100. [CrossRef]
41. Zhang, L.; You, T.; Zhou, T.; Zhou, X.; Xu, F. Interconnected Hierarchical Porous Carbon from Lignin-Derived Byproducts of Bioethanol Production for Ultra-High Performance Super capacitors. *ACS Appl. Mater. Interfaces* **2016**, *8*, 13918–13925. [CrossRef]
42. Han, K.; Yu, M. Study of the Preparation and Properties of UV-Blocking Fabrics of a PET/TiO_2 Nanocomposite Prepared by In Situ Polycondensation. *J. Appl. Polym. Sci.* **2006**, *100*, 1588–1593. [CrossRef]
43. Jiang, Y.; Song, Y.; Miao, M.; CaO, S.; Feng, X.; Fang, J.; Shi, L. Transparent nanocellulose hybrid films functionalized with ZnO nanostructures for UV-blocking. *J. Mater. Chem. C* **2015**, *3*, 6717–6724. [CrossRef]
44. Wang, R.H.; Xin, J.H.; Tao, X.M. UV-Blocking Property of Dumbbell-Shaped ZnO Crystallites on Cotton Fabrics. *Inorg. Chem.* **2005**, *44*, 3926–3930. [CrossRef] [PubMed]
45. Guo, D.; Zhang, J.; Sha, L.; Liu, B.; Zhang, X.; Zhang, X.; Xue, G. Preparation and characterization of lignin-TiO_2 UV-shielding composite material by induced synthesis with nanofibrillated cellulose. *BioResources* **2020**, *15*, 7374–7389. [CrossRef]
46. Shen, B.; Scaiano, J.C.; English, A.M. Zeolite Encapsulation Decreases TiO_2-photosensitized ROS Generation in Cultured Human Skin Fibroblasts. *Photochem. Photobiol.* **2006**, *82*, 5–12. [CrossRef]
47. Ibrahim, M.N.M.; Iqbal, A.; Shen, C.C.; Bhawani, S.A.; Adam, F. Synthesis of lignin based composites of TiO_2 for potential application as radical scavengers in sunscreen formulation. *BMC Chem.* **2019**, *13*, 17. [CrossRef]
48. Srisasiwimon, N.; Chuangchote, S.; Laosiripojana, N.; Sagawa, T. TiO_2/Lignin-Based Carbon Composited Photocatalysts for Enhanced Photocatalytic Conversion of Lignin to High Value Chemicals. *ACS Sustain. Chem. Eng.* **2018**, *6*, 13968–13976. [CrossRef]
49. Salimbeygi, G.; Nasouri, K.; Shoushtari, A.M.; Malek, R.; Mazaheri, F. Microwave Absorption Properties of Polyaniline/Poly(vinyl alcohol)/Multi-Walled Carbon Nanotube Composites in Thin Film and Nanofiber Layer Structures. *Macromol. Res.* **2015**, *23*, 741–748. [CrossRef]
50. Mondal, S.; Hu, J.L. A Novel Approach to Excellent UV Protecting Cotton Fabric with Functionalized MWNT Containing Water Vapor Permeable PU Coating. *J. Appl. Polym. Sci.* **2007**, *103*, 3370–3376. [CrossRef]
51. Nasouri, K.; Shoushtari, A.M.; Mirzaei, J.; Merati, A.A. Synthesis of carbon nanotubes composite nanofibers for ultrahigh performance UV protection and microwave absorption applications. *Diam. Relat. Mater.* **2020**, *107*, 107896. [CrossRef]
52. Mahmoudifard, M.; Safi, M. Novel study of carbon nanotubes as UV absorbers for the modification of cotton fabric. *J. Text. Inst.* **2012**, *103*, 893–899. [CrossRef]
53. Pnnusamy, V.K.; Nguyen, D.D.; Dharmaraja, J.; Shobana, S.; Banu, J.R.; Saratale, R.G.; Chang, S.W.; Kumar, G. A review on lignin structure, pretreatments, fermentation reactions and biorefinery potential. *Bioresour. Technol.* **2019**, *271*, 462–472. [CrossRef]
54. Li, Y.; Zhao, S.; Song, X.; Cao, D.; Li, K.; Hassanpour, M.; Zhang, Z. UV-Shielding Performance and Color of Lignin and its Application to Sunscreen. *Macromol. Mater. Eng.* **2022**, *307*, 2100628. [CrossRef]
55. Wang, J.; Deng, Y.; Qian, Y.; Qiu, X.; Ren, Y.; Yang, D. Reduction of lignin color via one-step UV irradiation. *Green Chem.* **2016**, *18*, 695–699. [CrossRef]
56. ATİK, C.; Balaban, M. Relation between CIE lab color values and the lignin content of Kraft pulps during bleaching. *Cellul. Chem. Technol.* **2003**, *37*, 385–389.

57. Qiu, X.; Yu, J.; Yang, D.; Wang, J.; Mo, W.; Qian, Y. Whitening sulfonated alkali lignin via H_2O_2/UV radiation and its application as dye dispersant. *ACS Sustain. Chem. Eng.* **2018**, *6*, 1055–1060. [CrossRef]
58. Zhang, H.; Fu, S.; Chen, Y. Basic understanding of the color distinction of lignin and the proper selection of lignin in color-depended utilizations. *Int. J. Biol. Macromol.* **2020**, *147*, 607–615. [CrossRef] [PubMed]
59. Lee, S.C.; Tran, T.M.T.; Choi, J.W.; Won, K. Lignin for white natural sunscreens. *Int. J. Biol. Macromol.* **2019**, *122*, 549–554. [CrossRef] [PubMed]
60. Qian, Y.; Zhong, X.; Li, Y.; Qiu, X. Fabrication of uniform lignin colloidal spheres for developing natural broad-spectrum sunscreens with high sun protection factor. *Ind. Crops Prod.* **2017**, *101*, 54–60. [CrossRef]
61. Widsten, P.; Tamminen, T.; Liitiä, T. Natural sunscreens based on nanoparticles of modified Kraft lignin (CatLignin). *ACS Omega* **2020**, *5*, 13438–13446. [CrossRef] [PubMed]
62. Lin, M.; Yang, L.; Zhang, H.; Xia, Y.; He, Y.; Lan, W.; Ren, J.; Yue, F.; Lu, F. Revealing the structure-activity relationship between lignin and anti-UV radiation. *Ind. Crops Prod.* **2021**, *174*, 114212. [CrossRef]
63. Wang, B.; Sun, D.; Wang, H.M.; Yuan, T.Q.; Sun, R.C. Green and facile preparation of regular lignin nanoparticles with high yield and their natural broad-spectrum sunscreens. *ACS Sustain. Chem. Eng.* **2018**, *7*, 2658–2666. [CrossRef]
64. Beisl, S.; Miltner, A.; Friedl, A. Lignin from micro-to nanosize: Production methods. *Int. J. Mol. Sci.* **2017**, *18*, 1244. [CrossRef] [PubMed]
65. Piccinino, D.; Capecchi, E.; Delfino, I.; Crucianelli, M.; Conte, N.; Avitabile, D.; Saladino, R. Green and Scalable Preparation of Colloidal Suspension of Lignin Nanoparticles and Its Application in Eco-friendly Sunscreen Formulations. *ACS Omega* **2021**, *6*, 21444–21456. [CrossRef]
66. Piccinino, D.; Capecchi, E.; Botta, L.; Bizzarri, B.M.; Bollella, P.; Antiochia, R.; Saladino, R. Layer-by-layer preparation of microcapsules and nanocapsules of mixed polyphenols with high antioxidant and UV-shielding properties. *Biomacromolecules* **2018**, *19*, 3883–3893. [CrossRef]
67. Xiong, F.; Han, Y.; Wang, S.; Li, G.; Qin, T.; Chen, Y.; Chu, F. Preparation and formation mechanism of size-controlled lignin nanospheres by self-assembly. *Ind. Crops Prod.* **2017**, *100*, 146–152. [CrossRef]
68. Fu, Y.; Qian, Y.; Zhang, A.; Lou, H.; Ouyang, X.; Yang, D.; Qiu, X. Long-Acting Ultraviolet-Blocking Mechanism of Lignin: Generation and Transformation of Semiquinone Radicals. *ACS Sustain. Chem. Eng.* **2022**, *10*, 5421–5429. [CrossRef]
69. Zhang, H.; Bai, Y.; Yu, B.; Liu, X.; Chen, F. A practicable process for lignin color reduction: Fractionation of lignin using methanol/water as a solvent. *Green Chem.* **2017**, *19*, 5152–5162. [CrossRef]
70. Zhang, H.; Liu, X.; Fu, S.; Chen, Y. Fabrication of light-colored lignin microspheres for developing natural sunscreens with favorable UV absorbability and staining resistance. *Ind. Eng. Chem. Res.* **2019**, *58*, 13858–13867. [CrossRef]
71. Trevisan, H.; Rezende, C.A. Pure, stable and highly antioxidant lignin nanoparticles from elephant grass. *Ind. Crops Prod.* **2020**, *145*, 112105. [CrossRef]
72. Li, R.; Huang, D.; Chen, S.; Lei, L.; Chen, Y.; Tao, J.; Zhou, W.; Wang, G. Insight into the self-assembly process of bamboo lignin purified by solvent fractionation to form uniform nanospheres with excellent UV resistance. *Colloids Surf. A Physicochem. Eng. Asp.* **2022**, *642*, 128652. [CrossRef]
73. Li, H.; Deng, Y.; Wu, H.; Ren, Y.; Qiu, X.; Zheng, D.; Li, C. Self-assembly of Kraft lignin into nanospheres in dioxane-water mixtures. *Holzforschung* **2016**, *70*, 725–731. [CrossRef]
74. Zhao, W.; Xiao, L.P.; Song, G.; Sun, R.C.; He, L.; Singh, S.; Simmons, B.A.; Cheng, G. From lignin subunits to aggregates: Insights into lignin solubilization. *Green Chem.* **2017**, *19*, 3272–3281. [CrossRef]
75. Qian, Y.; Deng, Y.; Qiu, X.; Li, H.; Yang, D. Formation of uniform colloidal spheres from lignin, a renewable resource recovered from pulping spent liquor. *Green Chem.* **2014**, *16*, 2156–2163. [CrossRef]
76. Gordobil, O.; Olaizola, P.; Banales, J.M.; Labidi, J. Lignins from agroindustrial by-products as natural ingredients for cosmetics: Chemical structure and in vitro sunscreen and cytotoxic activities. *Molecules* **2020**, *25*, 1131. [CrossRef]
77. Zhang, H.; Chen, F.; Liu, X.; Fu, S. Micromorphology influence on the color performance of lignin and its application in guiding the preparation of light-colored lignin sunscreen. *ACS Sustain. Chem. Eng.* **2018**, *6*, 12532–12540. [CrossRef]
78. de Araújo Padilha, C.E.; da Costa Nogueira, C.; Oliveira Filho, M.A.; de Santana Souza, D.F.; de Oliveira, J.A.; dos Santos, E.S. Valorization of cashew apple bagasse using acetic acid pretreatment: Production of cellulosic ethanol and lignin for their use as sunscreen ingredients. *Process Biochem.* **2020**, *91*, 23–33. [CrossRef]
79. Qiu, X.; Li, Y.; Qian, Y.; Wang, J.; Zhu, S. Long-acting and safe sunscreens with ultrahigh sun protection factor via natural lignin encapsulation and synergy. *ACS Appl. Bio Mater.* **2018**, *1*, 1276–1285. [CrossRef]
80. Kim, J.Y.; Hwang, H.; Oh, S.; Kim, Y.S.; Kim, U.J.; Choi, J.W. Investigation of structural modification and thermal characteristics of lignin after heat treatment. *Int. J. Biol. Macromol.* **2014**, *66*, 57–65. [CrossRef]
81. Chen, Y.; Fan, Y.; Gao, J.; Li, H. Coloring characteristics of in situ lignin during heat treatment. *Wood Sci. Technol.* **2012**, *46*, 33–40.
82. Björkman, A. Lignin and lignin-carbohydrate complexes: Extraction from wood meal with neutral solvents. *Ind. Eng. Chem.* **1957**, *49*, 1395–1398. [CrossRef]
83. Constant, S.; Wienk, H.L.J.; Frissen, A.E.; de Peinder, P.; Boelens, R.; van Es, D.S.; Grisel, R.J.H.; Weckhuysen, B.M.; Huijgen, W.J.J.; Gosselink, R.J.A.; et al. New insights into the structure and composition of technical lignins: A comparative characterization study. *Green Chem.* **2016**, *18*, 2651–2665. [CrossRef]

84. Zhang, Y.; Yang, L.; Wang, D.; Li, D. Structure elucidation and properties of different lignins isolated from acorn shell of Quercus variabilis Bl. *Int. J. Biol. Macromol.* **2018**, *107*, 1193–1202. [CrossRef] [PubMed]
85. Zhang, H.; Liu, X.; Fu, S.; Chen, Y. High-value utilization of Kraft lignin: Color reduction and evaluation as sunscreen ingredient. *Int. J. Biol. Macromol.* **2019**, *133*, 86–92. [CrossRef]
86. Imsgard, F.; Falkehag, S.I.; Kringstad, K.P. *On Possible Chromophoric Structures in Spruce Wood*; Technical Association of the Pulp & Paper Industry Inc.: Peachtree Corners, GA, USA, 1971.
87. Zakis, G.F.; Melkis, A.A.; Nieberte, B.Y. Methods for determination of quinone carbonyl groups in lignins. *Khim Drev.* **1987**, *3*, 82–86.
88. Argyropoulos, D.S.; Heitner, C. 31P NMR spectroscopy in wood chemistry. Part VI. Solid state 31P NMR of trimethyl phosphite derivatives of chromophores and carboxylic acids present in mechanical pulps; a method for the quantitative determination of ortho-quinones. *Holzforschung* **1994**, *48*, 112–116. [CrossRef]
89. Buranov, A.U.; Mazza, G. Lignin in straw of herbaceous crops. *Ind. Crops Prod.* **2008**, *28*, 237–259. [CrossRef]
90. Schutyser, W.; Renders, A.T.; Van den Bosch, S.; Koelewijn, S.F.; Beckham, G.T.; Sels, B.F. Chemicals from lignin: An interplay of lignocellulose fractionation, depolymerisation, and upgrading. *Chem. Soc. Rev.* **2018**, *47*, 852–908. [CrossRef]
91. Kazzaz, A.E.; Fatehi, P. Technical lignin and its potential modification routes: A mini-review. *Ind. Crops Prod.* **2020**, *154*, 112732. [CrossRef]
92. Chio, C.; Sain, M.; Qin, W. Lignin utilization: A review of lignin depolymerization from various aspects. *Renew. Sustain. Energy Rev.* **2019**, *107*, 232–249. [CrossRef]
93. Darmawan, M.A.; Ramadhani, N.H.; Hubeis, N.A.; Ramadhan, M.Y.A.; Sahlan, M.; Abd-Aziz, S.; Gozan, M. Natural sunscreen formulation with a high sun protection factor (SPF) from tengkawang butter and lignin. *Ind. Crops Prod.* **2022**, *177*, 114466. [CrossRef]
94. Hambardzumyan, A.; Foulon, L.; Chabbert, B.; Aguié-Béghin, V. Natural Organic UV-Absorbent Coatings Based on Cellulose and Lignin: Designed Effects on Spectroscopic Properties. *Biomacromolecules* **2012**, *13*, 4081–4088. [CrossRef] [PubMed]
95. Moon, R.J.; Martini, A.; Nairn, J.; Simonsen, J.; Youngblood, J. Cellulose nanomaterials review: Structure, properties and nanocomposites. *Chem. Soc. Rev.* **2011**, *40*, 3941–3994. [CrossRef] [PubMed]
96. Jung, K.Y.; Park, S.B. Anatase-phase titania: Preparation by embedding silica and photocatalytic activity for the decomposition of trichloroethylene. *J. Photochem. Photobiol. A* **1999**, *127*, 117–122. [CrossRef]
97. Jaroenworaluck, A.; Sunsaneeyametha, W.; Kosachan, N.; Steven, R. Characteristics of silica-coated TiO_2 and its UV absorption for sunscreen cosmetic applications. *Surf. Interface Anal.* **2006**, *38*, 473–477. [CrossRef]
98. Jeelani, P.G.; Mulay, P.; Venkat, R.; Ramalingam, C. Multifaceted application of silica nanoparticles. A review. *Silicon* **2020**, *12*, 1337–1354. [CrossRef]
99. Alarcos, N.; Cohen, B.; Ziółek, M.; Douhal, A. Photochemistry and photophysics in silica-based materials: Ultrafast and single molecule spectroscopy observation. *Chem. Rev.* **2017**, *117*, 13639–13720. [CrossRef] [PubMed]
100. Wang, Y.; Zhao, Q.; Han, N.; Bai, L.; Li, J.; Liu, J.; Che, E.; Hu, L.; Zhang, Q.; Jiang, T.; et al. Mesoporous silica nanoparticles in drug delivery and biomedical applications. *Nanomedicine* **2015**, *11*, 313–327. [CrossRef]
101. Kilpeläinen, M.; Riikonen, J.; Vlasova, M.A.; Huotari, A.; Lehto, V.P.; Salonen, J.; Herzig, K.H.; Järvinen, K. In vivo delivery of a peptide, ghrelin antagonist, with mesoporous silicon microparticles. *J. Control Release* **2009**, *137*, 166–170. [CrossRef] [PubMed]
102. Olivieri, F.; Castaldo, R.; Cocca, M.; Gentile, G.; Lavorgna, M. Mesoporous silica nanoparticles as carriers of active agents for smart anticorrosive organic coatings: A critical review. *Nanoscale* **2021**, *13*, 9091–9111. [CrossRef]
103. Wu, Z.; Zhao, D. Ordered mesoporous materials as adsorbents. *Chem. Commun.* **2011**, *47*, 3332–3338. [CrossRef]
104. Castaldo, R.; Gentile, G.; Avella, M.; Carfagna, C.; Ambrogi, V. Microporous hyper-crosslinked polystyrenes and nanocomposites with high adsorption properties: A review. *Polymers* **2017**, *9*, 651. [CrossRef] [PubMed]
105. Hu, X.; Wang, Y.; Peng, B. Chitosan-capped mesoporous silica nanoparticles as pH-responsive nanocarriers for controlled drug release. *Chem. Asian J.* **2014**, *9*, 319–327. [CrossRef]
106. Liu, X.; Li, W.; Wang, W.; Song, L.; Fan, W.; Gao, X.; Xiong, C. Synthesis and characterization of pH-responsive mesoporous chitosan microspheres loaded with sodium phytate for smart water-based coatings. *Mater. Corros.* **2018**, *69*, 736–748. [CrossRef]
107. Azizi Samir, M.A.S.; Alloin, F.; Dufresne, A. Review of recent research into cellulosic whiskers, their properties and their application in nanocomposite field. *Biomacromolecules* **2005**, *6*, 612–626. [CrossRef] [PubMed]
108. Sharma, A.; Thakur, M.; Bhattacharya, M.; Mandal, T.; Goswami, S. Commercial application of cellulose nano-composites–A review. *Biotechnol. Rep.* **2019**, *21*, e00316. [CrossRef]
109. Phanthong, P.; Reubroycharoen, P.; Hao, X.; Xu, G.; Abudula, A.; Guan, G. Nanocellulose: Extraction and application. *Carbon Resour. Convers.* **2018**, *1*, 32–43. [CrossRef]
110. Garcia de Rodriguez, N.L.; Thielemans, W.; Dufresne, A. Sisal cellulose whiskers reinforced polyvinyl acetate nanocomposites. *Cellulose* **2006**, *13*, 261–270. [CrossRef]
111. Beck-Candanedo, S.; Roman, M.; Gray, D.G. Effect of reaction conditions on the properties and behavior of wood cellulose nanocrystal suspensions. *Biomacromolecules* **2005**, *6*, 1048–1054. [CrossRef]
112. Bai, W.; Holbery, J.; Li, K. A technique for production of nanocrystalline cellulose with a narrow size distribution. *Cellulose* **2009**, *16*, 455–465. [CrossRef]

113. Klemm, D.; Kramer, F.; Moritz, S.; Lindström, T.; Ankerfors, M.; Gray, D.; Dorris, A. Nanocelluloses: A new family of nature-based materials. *Angew. Chem. Int. Ed.* **2011**, *50*, 5438–5466. [CrossRef]
114. Dufresne, A. Nanocellulose: A new ageless bionanomaterial. *Mater. Today* **2013**, *16*, 220–227. [CrossRef]
115. Khalil, H.A.; Bhat, A.H.; Yusra, A.I. Green composites from sustainable cellulose nanofibrils: A review. *Carbohydr. Polym.* **2012**, *87*, 963–979. [CrossRef]
116. Ferrer, A.; Pal, L.; Hubbe, M. Nanocellulose in packaging: Advances in barrier layer technologies. *Ind. Crops Prod.* **2017**, *95*, 574–582. [CrossRef]
117. Jaroenworaluck, A.; Pijarn, N.; Kosachan, N.; Stevens, R. Nanocomposite TiO_2–SiO_2 gel for UV absorption. *Chem. Eng. J.* **2012**, *181*, 45–55. [CrossRef]
118. Sotiriou, G.A.; Watson, C.; Murdaugh, K.M.; Darrah, T.H.; Pyrgiotakis, G.; Elder, A.; Brain, J.D.; Demokritou, P. Engineering safer-by-design silica-coated ZnO nanorods with reduced DNA damage potential. *Environ. Sci. Nano* **2014**, *1*, 144–153. [CrossRef] [PubMed]
119. Li, C.C.; Chen, Y.T.; Lin, Y.T.; Sie, S.F.; Chen-Yang, Y.W. Mesoporous silica aerogel as a drug carrier for the enhancement of the sunscreen ability of benzophenone-3. *Colloids Surf. B.* **2014**, *115*, 191–196. [CrossRef] [PubMed]
120. Olson, E.; Li, Y.; Lin, F.Y.; Miller, A.; Liu, F.; Tsyrenova, A.; Palm, D.; Curtzwiler, G.W.; Vorst, K.L.; Cochran, E.; et al. Thin biobased transparent UV-blocking coating enabled by nanoparticle self-assembly. *ACS Appl. Mater. Interfaces* **2019**, *11*, 24552–24559. [CrossRef]
121. Yuying, P.U.; Jianzhang, F.A.N.G.; Feng, P.E.N.G.; Baojian, L.I.; Huang, L. Microemulsion synthesis of nanosized SiO_2/TiO_2 particles and their photocatalytic activity. *Chin. J. Catal.* **2007**, *28*, 251–256.
122. Linsebigler, A.L.; Lu, G.; Yates, J.T., Jr. Photocatalysis on TiO^2 surfaces: Principles, mechanisms, and selected results. *Chem. Rev.* **1995**, *95*, 735–758. [CrossRef]
123. Serpone, N.; Dondi, D.; Albini, A. Inorganic and organic UV filters: Their role and efficacy in sunscreens and suncare products. *Inorg. Chim. Acta* **2007**, *360*, 794–802. [CrossRef]
124. Kullavanijaya, P.; Lim, H.W. Photoprotection. *J. Am Acad. Dermatol.* **2005**, *52*, 937–958. [CrossRef]
125. Murphy, G.M. Sunblocks: Mechanisms of action. *Photodermatol. Photoimmunol. Photomed.* **1999**, *15*, 34–36. [CrossRef] [PubMed]
126. Reidy, D.J.; Holmes, J.D.; Morris, M.A. Preparation of a highly thermally stable titania anatase phase by addition of mixed zirconia and silica dopants. *Ceram. Int.* **2006**, *32*, 235–239. [CrossRef]
127. Anderson, C.; Bard, A.J. Improved photocatalytic activity and characterization of mixed TiO_2/SiO_2 and TiO_2/Al_2O_3 materials. *J. Phys. Chem. B* **1997**, *101*, 2611–2616. [CrossRef]
128. Morawski, A.W.; Kusiak-Nejman, E.; Przepiórski, J.; Kordala, R.; Pernak, J. Cellulose-TiO_2 nanocomposite with enhanced UV–Vis light absorption. *Cellulose* **2013**, *20*, 1293–1300. [CrossRef]
129. Abdalkarim, S.Y.H.; Yu, H.Y.; Wang, C.; Yang, L.; Guan, Y.; Huang, L.; Yao, J. Sheet-like cellulose nanocrystal-ZnO nanohybrids as multifunctional reinforcing agents in biopolyester composite nanofibers with ultrahigh UV-shielding and antibacterial performances. *ACS Appl. Bio Mater.* **2018**, *1*, 714–727. [CrossRef]
130. Gasparro, F.P.; Mitchnick, M.; Nash, J.F. A review of sunscreen safety and efficacy. *Photochem. Photobiol.* **1998**, *68*, 243–256. [CrossRef]
131. Yoo, J.; Kim, H.; Chang, H.; Park, W.; Hahn, S.K.; Kwon, W. Biocompatible organosilica nanoparticles with self-encapsulated phenyl motifs for effective UV protection. *ACS Appl. Mater. Interfaces* **2020**, *12*, 9062–9069. [CrossRef]
132. Setlow, R.B.; Grist, E.; Thompson, K.; Woodhead, A.D. Wavelengths effective in induction of malignant melanoma. *Proc. Natl. Acad. Sci. USA* **1993**, *90*, 6666–6670. [CrossRef]
133. Walenzyk, T.; Carola, C.; Buchholz, H.; König, B. Synthesis of mono-dispersed spherical silica particles containing covalently bonded chromophores. *Int. J. Cosmet. Sci.* **2005**, *27*, 177–189. [CrossRef]
134. Knežević, N.Z.; Ilić, N.; Đokić, V.; Petrović, R.; Janaćković, D. Mesoporous silica and organosilica nanomaterials as UV-blocking agents. *ACS Appl. Mater. Interfaces* **2018**, *10*, 20231–20236. [CrossRef]
135. Sun, H.; Liu, Y.; Guo, X.; Zeng, K.; Mondal, A.K.; Li, J.; Tao, Y.; Chen, L. Strong, robust cellulose composite film for efficient light management in energy efficient building. *Chem. Eng. J.* **2021**, *425*, 131469. [CrossRef]
136. Sirviö, J.A.; Visanko, M.; Heiskanen, J.P.; Liimatainen, H. UV-absorbing cellulose nanocrystals as functional reinforcing fillers in polymer nanocomposite films. *J. Mater. Cem. A* **2016**, *4*, 6368–6375. [CrossRef]
137. Baccile, N.; Babonneau, F.; Thomas, B.; Coradin, T. Introducing ecodesign in silica sol–gel materials. *J. Mater. Chem.* **2009**, *19*, 8537–8559. [CrossRef]
138. Laine, R.M.; Blohowiak, K.Y.; Robinson, T.R.; Hoppe, M.L.; Nardi, P.; Kampf, J.; Uhm, J. Synthesis of pentacoordinate silicon complexes from SiO_2. *Nature* **1991**, *353*, 642–644. [CrossRef]
139. Pode, R. Potential applications of rice husk ash waste from rice husk biomass power plant. *Renew. Sustain. Energy Rev.* **2016**, *53*, 1468–1485. [CrossRef]
140. Chen, H.; Wang, W.; Martin, J.C.; Oliphant, A.J.; Xu, J.F.; DeBorn, K.M.; Chen, C.; Sun, L. Extraction of lignocellulose and synthesis of porous silica nanoparticles from rice husks: A comprehensive utilization of rice husk biomass. *ACS Sustain. Chem. Eng.* **2013**, *1*, 254–259. [CrossRef]
141. Wang, W.; Martin, J.C.; Fan, X.; Han, A.; Luo, Z.; Sun, L. Silica nanoparticles and frameworks from rice husk biomass. *ACS Appl. Mater. Interfaces* **2012**, *4*, 977–981. [CrossRef]

142. Della, V.P.; Kühn, I.; Hotza, D. Rice husk ash as an alternate source for active silica production. *Mater. Lett.* **2002**, *57*, 818–821. [CrossRef]
143. Wang, Z.; Zeng, S.; Joshi, G.N.; Smith, A.T.; Zeng, H.; Wei, Z.; Yu, X.; Pokhrel, M.; Mao, Y.; Wang, W.; et al. Design and fabrication of highly photoluminescent carbon-incorporated silica from rice husk biomass. *Ind. Eng. Chem. Res.* **2019**, *58*, 4688–4694. [CrossRef]
144. Yang, W.; Feng, Y.; He, H.; Yang, Z. Environmentally-friendly extraction of cellulose nanofibers from steam-explosion pretreated sugar beet pulp. *Materials* **2018**, *11*, 1160. [CrossRef] [PubMed]
145. Dilamian, M.; Noroozi, B. A combined homogenization-high intensity ultrasonication process for individualizaion of cellulose micro-nano fibers from rice straw. *Cellulose* **2019**, *26*, 5831–5849. [CrossRef]
146. Sofla, M.R.K.; Brown, R.J.; Tsuzuki, T.; Rainey, T.J. A comparison of cellulose nanocrystals and cellulose nanofibres extracted from bagasse using acid and ball milling methods. *Adv. Nat. Sci. Nanosci. Nanotechnol.* **2016**, *7*, 035004. [CrossRef]
147. Peart, C.; Ni, Y. UV-Vis spectra of lignin model compounds in the presence of metal ions and chelants. *J. Wood Chem. Technol.* **2001**, *21*, 113–125. [CrossRef]
148. McCarthy, J.L.; Islam, A. Lignin chemistry, technology, and utilization: A brief history. *ACS Symp. Ser.* **1999**, *742*, 2–66.
149. Li, S.X.; Li, M.F.; Bian, J.; Wu, X.F.; Peng, M.; Ma, M.G. Preparation of organic acid lignin submicrometer particle as a natural broad-spectrum photo-protection agent. *Int. J. Biol. Macromol.* **2019**, *132*, 836–843. [CrossRef]
150. Wu, Y.; Qian, Y.; Lou, H.; Yang, D.; Qiu, X. Enhancing the Broad-Spectrum Adsorption of Lignin through Methoxyl Activation, Grafting Modification, and Reverse Self-Assembly. *ACS Sustain. Chem. Eng.* **2019**, *7*, 15966–15973. [CrossRef]
151. Shi, C.; Zhang, S.; Wang, W.; Linhardt, R.J.; Ragauskas, A.J. Preparation of Highly Reactive Lignin by Ozone Oxidation: Application as Surfactants with Antioxidant and Anti-UV Properties. *ACS Sustain. Chem. Eng.* **2020**, *8*, 22–28. [CrossRef]
152. Paulsson, M.; Parkås, J. Review: Light-induced yellowing of lignocellulosic pulps—Mechanisms and preventive methods. *BioResources* **2012**, *7*, 5995–6040. [CrossRef]
153. DiFonzo, N.; Bordia, P. Peroxidations initiated by lignin model compounds: Investigating the role of singlet oxygen in photo-yellowing. *J. Allergy Clin. Immunol.* **1998**, *130*, 556.
154. Yu, J.; Li, L.; Qian, Y.; Lou, H.; Yang, D.; Qiu, X. Facile and Green Preparation of High UV-Blocking Lignin/Titanium Dioxide Nanocomposites for Developing Natural Sunscreens. *Ind. Eng. Chem. Res.* **2018**, *57*, 15740–15748. [CrossRef]
155. Gutiérrez-Hernández, J.M.; Escalante, A.; Murillo-Vázquez, R.N.; Delgado, E.; González, F.J.; Toríz, G. Use of Agave tequilana-lignin and zinc oxide nanoparticles for skin photoprotection. *J. Photochem. Photobiol. B Biol.* **2016**, *163*, 156–161. [CrossRef] [PubMed]
156. Lim, J.; Sana, B.; Krishnan, R.; Seayad, J.; Ghadessy, F.J.; Jana, S.; Ramalingam, B. Laccase-catalyzed synthesis of low-molecular-weight lignin-like oligomers and their application as UV-blocking materials. *Chem. Asian J.* **2018**, *13*, 284–291. [CrossRef] [PubMed]
157. Avelino, F.; de Oliveira, D.R.; Mazzetto, S.E.; Lomonaco, D. Poly(methyl methacrylate) films reinforced with coconut shell lignin fractions to enhance their UV-blocking, antioxidant and thermo-mechanical properties. *Int. J. Biol. Macromol.* **2019**, *125*, 171–180. [CrossRef]
158. Xing, Q.; Ruch, D.; Dubois, P.; Wu, L.; Wang, W.J. Biodegradable and High-Performance Poly(butylene adipate-co-terephthalate)-Lignin UV-Blocking Films. *ACS Sustain. Chem. Eng.* **2017**, *5*, 10342–10351. [CrossRef]
159. Lee, E.; Song, Y.; Lee, S. Crosslinking of lignin/poly(vinyl alcohol) nanocomposite fiber webs and their antimicrobial and ultraviolet-protective properties. *Text. Res. J.* **2019**, *89*, 3–12. [CrossRef]
160. He, X.; Luzi, F.; Hao, X.; Yang, W.; Torre, L.; Xiao, Z.; Xie, Y.; Puglia, D. Thermal, antioxidant and swelling behaviour of transparent polyvinyl (alcohol) films in presence of hydrophobic citric acid-modified lignin nanoparticles. *Int. J. Biol. Macromol.* **2019**, *127*, 665–676. [CrossRef]
161. Wu, W.; Liu, T.; Deng, X.; Sun, Q.; Cao, X.; Feng, Y.; Wang, B.; Roy, V.A.L.; Li, R.K. Ecofriendly UV-protective films based on poly (propylene carbonate) biocomposites filled with TiO_2 decorated lignin. *Int. J. Biol. Macromol.* **2019**, *126*, 1030–1036. [CrossRef]
162. Rukmanikrishnan, B.; Ramalingam, S.; Rajasekharan, S.K.; Lee, J.; Lee, J. Binary and ternary sustainable composites of gellan gum, hydroxyethyl cellulose and lignin for food packaging applications: Biocompatibility, antioxidant activity, UV and water barrier properties. *Int. J. Biol. Macromol.* **2020**, *153*, 55–62. [CrossRef]
163. Kim, Y.; Suhr, J.; Seo, H.W.; Sun, H.; Kim, S.; Park, I.K.; Kim, S.H.; Lee, Y.K.; Kim, K.J.; Nam, J.D. All biomass and UV protective composite composed of compatibilized lignin and poly (lactic-acid). *Sci. Rep.* **2017**, *7*, 43596. [CrossRef]
164. Shikinaka, K.; Nakamura, M.; Navarro, R.R.; Otsuka, Y. Non-flammable and moisture-permeable UV protection films only from plant polymers and clay minerals. *Green Chem.* **2019**, *21*, 498–502. [CrossRef]
165. Chen, K.; Qian, Y.; Wu, S.; Qiu, X.; Yang, D.; Lei, L. Neutral fabrication of UV-blocking and antioxidation lignin-stabilized high internal phase emulsion encapsulates for high efficient antibacterium of natural curcumin. *Food Funct.* **2019**, *10*, 3543–3555. [CrossRef]
166. Yuan, M.; Liu, H.; Shen, K.; Qiu, C.; Qi, H. Transparent cellulose-based film with high UV-blocking performance fabricated by surface modification using Biginelli reaction. *Macromol. Rapid Commun.* **2022**, *2200495*, 2200495. [CrossRef] [PubMed]
167. Zhang, X.; Li, Y.; Guo, M.; Jin, T.Z.; Arabi, S.A.; He, Q.; Ismail, B.B.; Hu, Y.; Liu, D. Antimicrobial and UV blocking properties of composite chitosan films with curcumin grafted cellulose nanofiber. *Food Hydrocoll.* **2021**, *112*, 106337. [CrossRef]

168. Mendoza, D.J.; Browne, C.; Raghuwanshi, V.S.; Mouterde, L.M.; Simon, G.P.; Allais, F.; Garnier, G. Phenolic ester-decorated cellulose nanocrystals as UV-absorbing nanoreinforcements in polyvinyl alcohol films. *ACS Sustain. Chem. Eng.* **2021**, *9*, 6427–6437. [CrossRef]
169. Feng, Z.; Xu, D.; Shao, Z.; Zhu, P.; Qiu, J.; Zhu, L. Rice straw cellulose microfiber reinforcing PVA composite film of ultraviolet blocking through pre-cross-linking. *Carbohydr. Polym.* **2022**, *296*, 119886. [CrossRef] [PubMed]
170. Sánchez-Quiles, D.; Tovar-Sánchez, A. Are sunscreens a new environmental risk associated with coastal tourism? *Environ. Int.* **2015**, *83*, 158–170. [CrossRef] [PubMed]
171. Grande, F.; Tucci, P. Titanium dioxide nanoparticles: A risk for human health? *Mini Rev. Med. Chem.* **2016**, *16*, 762–769. [CrossRef]
172. Xia, T.; Kovochich, M.; Liong, M.; Mädler, L.; Gilbert, B.; Shi, H.; Yeh, J.I.; Zink, J.I.; Nel, A.E. Comparison of the mechanism of toxicity of zinc oxide and cerium oxide nanoparticles based on dissolution and oxidative stress properties. *ACS Nano* **2008**, *2*, 2121–2134. [CrossRef]
173. Prabha, S.; Durgalakshmi, D.; Rajendran, S.; Lichtfouse, E. Plant-derived silica nanoparticles and composites for biosensors, bioimaging, drug delivery and supercapacitors: A review. *Environ. Chem. Lett.* **2021**, *19*, 1667–1691. [CrossRef]
174. Zhang, J.; Raphael, A.P.; Yang, Y.; Popat, A.; Prow, T.W.; Yu, C. Nanodispersed UV blockers in skin-friendly silica vesicles with superior UV-attenuating efficiency. *J. Mater. Chem. B* **2014**, *2*, 7673–7678. [CrossRef] [PubMed]
175. Chen-Yang, Y.W.; Chen, Y.T.; Li, C.C.; Yu, H.C.; Chuang, Y.C.; Su, J.H.; Lin, Y.T. Preparation of UV-filter encapsulated mesoporous silica with high sunscreen ability. *Mater. Lett.* **2011**, *65*, 1060–1062. [CrossRef]
176. Choi, S.; Kim, J.; Rahman, R.T.; Lee, D.J.; Lee, K.; Nam, Y.S. Plastic-free silica-titania-polyphenol heterojunction hybrids for efficient UV-to-blue light blocking and suppressed photochemical reactivity. *Chem. Eng. J.* **2022**, *431*, 133790. [CrossRef]
177. Fagervold, S.K.; Rodrigues, A.S.; Rohée, C.; Roe, R.; Bourrain, M.; Stien, D.; Lebaron, P. Occurrence and environmental distribution of 5 UV filters during the summer season in different water bodies. *Water Air Soil Pollut.* **2019**, *230*, 172. [CrossRef]
178. Dransfield, G.P. Inorganic sunscreens. *Radiat. Prot. Dosim.* **2000**, *91*, 271–273. [CrossRef]
179. Surber, C.; Plautz, J.; Dähnhardt-Pfeiffer, S.; Osterwalder, U. Size matters! Issues and challenges with nanoparticulate UV filters. *Chall. Sun Prot.* **2021**, *55*, 203–222.
180. Abbas, N.; Manzoor, S.; Saeed, S.; Husnain, S.M.; Tariq, M.; Akhtar, Z.; Saira, N.; Yasmin, G. Investigation of calcium silicate as a natural clay-based sunblock: Formulation and characterization. *Photodermatol. Photoimmunol. Photomed.* **2021**, *37*, 39–48. [CrossRef] [PubMed]
181. Cheraghian, G.; Wistuba, M.P. Effect of fumed silica nanoparticles on ultraviolet aging resistance of bitumen. *Nanomaterials* **2021**, *11*, 454. [CrossRef]